Universidad
Carlos III de Madrid

DOCTORAL THESIS

# BLOCK DIAGONALIZATION TECHNIQUES FOR CELLULAR NETWORKS: CLUSTERING AND SCHEDULING

Author: JUAN JOSÉ GARCÍA FERNÁNDEZ

Advisor: ANA GARCÍA ARMADA

Departamento de Teoría de la Señal y Comunicaciones

Leganés, June 2015

| | |
|---|---|
| **Tesis Doctoral:** | BLOCK DIAGONALIZATION TECHNIQUES FOR CELLULAR NETWORKS: CLUSTERING AND SCHEDULING |
| **Autor:** | Juan José García Fernández |
| **Director:** | Dra. Ana García Armada |

El tribunal nombrado para juzgar la tesis doctoral arriba citada, compuesto por los doctores

Presidente:

Vocal:

Secretario:

acuerda otorgarle la calificación de

Leganés, a

# Agradecimientos

Mi primer y más importante agradecimiento va dirigido a mis padres. Por respetar mis erráticos pasos por este mundo, incluso cuando no los compartían. Siempre han estado ahí, como un contrafuerte sobre el que apoyar la carga de las preocupaciones, cuando ha sido necesario. Mi hermana, en la distancia, también ha sido participe de que sea como soy y quien soy ahora mismo. Ella pasó por lo mismo pero, como siempre le ha ocurrido, sin un hermano mayor a quien recurrir, haciéndolo más difícil. Gracias a ellos, llegar a este punto no ha sido tan difícil como me gusta decir.

Y es que me he quejado mucho durante este tiempo, pero como dicen mis amigos los pollos, "he vivido como he querido". En los últimos tiempos me he distanciado de ellos, pero sé que siempre están ahí si realmente necesito algo de ellos, de forma desinteresada, por ello quiero darles las gracias.

No me puedo olvidar, aunque lo había hecho, de Julio, José y Rober (y Bea cuando se digna), que con esporádicos frikimiércoles han mantenido viva la chispa de la curiosidad por cosas diferentes, cada uno hablándonos de nuestras cosas.

Por supuesto, con quien más tiempo he pasado, al final, ha sido con mis compañeros de laboratorio, Máximo, Özge, Javier, Alex, Alex (el orden lo elegís vosotros), Borja, Cecilia. En el fondo son la principal razón por la que merecía la pena ir cada día a la universidad. Antes que todos ellos, Omar estuvo ahí, y juntos compartimos penurias y lamentos, de los que espero que nos vayamos librando poco a poco. A tita Sara tengo que agradecerle su optimismo resignado, siempre enfrentándose a la dura realidad con una visión positiva. Lo mejor es que ahora volveré a compartir tiempo con ella... un aliciente más para afrontar el siguiente paso. Con un optimismo ligeramente diferente, Jair siempre ha servido de motivación para seguir adelante. Su visión del mundo de la universidad realmente llegaba a calar, y me hizo comprender, en ocasiones, que no todo era tan negro como lo veía.

A mi tutora, Ana, he de agradecerle su optimismo infatigable y su capacidad para ver lo bueno en todo, y por su paciencia aguantándome.

During the time I spent in the USA, I met very special people. First I want to thank Nima and Tommi, because they were (and still are, from afar) true friends, and made

the life much easier in there. It is always a relief finding people who are so similar to me, so far from home. Meo appeared at some point, too, with her capacity to joke about almost anything, but still be serious when needed. And she appeared through the most special person I met there, Samar. I spent with her the most precious time I have spent with anyone in the recent years. Despite the distance, she is still so important for me. I want to thank her because she was the main reason to continue with the PhD, her selfless support kept me focused and gave me strength to not give up. I want to truly thank her for having so much faith in me.

Aparte de los compañeros de laboratorio, las actividades deportivas han sido otro de los pilares que me han mantenido en pie. La natación y el aikido me han dado la vida, a través de la salud. A mis monitores de natación (Jesús y Gema), y a mi sensei (Julio) he de agradecerles sus esfuerzos. Y a mis compañeros de aikido Borja, Gerardo, Javier y Rodolfo, agradecerles la posibilidad de entrenar y crecer juntos.

Finalmente quiero agradecer el apoyo recibido de múltiples otros amigos y amigas, que con el tiempo que me han dedicado han conseguido que pudiera respirar a través de las brumas del desánimo. Unos más recientes, otros más antiguos, su aportación ha sido igualmente importante: Carlos, Diego, Esther, Isaac, Lydia, Marcos.

# Abstract

The need for higher data rates and higher efficiency in cellular networks motivates the use of Universal Frequency Reuse (UFR). Coordination among Base Stations (BSs) is required then to alleviate the performance penalty due to the interference. Global coordination is too complex and has inherent limitations that prevents it from being used in real world scenarios. Clusters of a reduced number of BSs can be considered in order to ease off the requirements of coordination. As a result, Other Cluster Interference (OCI) appears, affecting negatively the communications.

This work focuses on Block Diagonalization (BD), a linear precoding technique that combines a good theoretical performance with a relatively low complexity. However, the unwanted interference seriously impacts the results obtained using BD.

This thesis studies the downlink of a clustered cellular network, where BD is used to coordinate the BS within each cluster. The mean achievable rate is analyzed as a function of several scenario parameters. Of particular interest is the dependence on the cluster size, which yields that there is an optimum cluster size, beyond which no significant gain is obtained. Fairness considerations are analyzed in the presence of OCI, also studied as a function of scenario parameters such as the power allocation.

A mixed strategy using BD and Single User (SU) processing is proposed as a means to overcome the impairment of the unhandled interference. The transmission consists of two stages:

- Users locally decide which transmission strategy they prefer and send this information to the BSs.
- BSs use the decisions of all users to schedule them for transmission so that the performance of the network is optimized.

The result of the proposed strategy is an improvement in the performance of BD in the presence of OCI, especially for the users experiencing the worst conditions. This means that the fairness of the system is also increased, along with the overall performance of the network.

# Resumen

La necesidad de tasas de transmisión más elevadas y una mayor eficiencia en las redes celulares es la principal motivación para considerar el uso de UFR. La coordinación entre BSs se hace necesaria, entonces, para compensar los problemas introducidos por la interferencia. La coordinación global de la red es demasiado compleja y, además, presenta limitaciones intrínsecas, que impiden su utilización en escenarios reales. La utilización de grupos reducidos de BSs es una alternativa para reducir los requisitos impuestos por la coordinación. Como consecuencia de la agrupación, aparece OCI, la cual perjudica seriamente las comunicaciones.

Este trabajo se centra en BD, una técnica de precodificación lineal que combina unas buenas prestaciones con una complejidad relativamente baja. Sin embargo, la interferencia empeora notablemente su funcionamiento.

En esta tesis se estudia el canal descendente de una red celular conglomerada, donde se usa BD para coordinar las BSs que forman cada grupo. Se analiza la tasa media obtenible como función de múltiples parámetros del escenario. De especial interés es la dependencia con el tamaño de las agrupaciones, de donde se desprende que existe un tamaño óptimo para los grupos de BSs, por encima del cual no se obtienen mejoras significativas. La equidad del sistema se estudia en presencia de OCI, también como función de diversos parámetros del escenario, como puede ser la asignación de potencia.

Se propone una estrategia mixta de transmisión, que combina BD con procesado SU, como mecanismo para combatir las dificultades introducidas por la interferencia que no se gestiona. La estrategia consiste en dos fases:

- Los usuarios deciden localmente qué estrategia prefieren para la transmisión, y envían esta información a las BSs.
- Las BSs utilizan las decisiones recibidas para planificar las transmisiones, de modo que se pueda optimizar el funcionamiento de la red.

El resultado de la estrategia propuesta es una mejora de las prestaciones de BD en presencia de OCI, especialmente para los usuarios más desfavorecidos. Esto se traduce en que, adicionalmente, el sistema se vuelve más justo, al mismo tiempo que el rendimiento de la red aumenta.

# Contents

# List of Figures

# Notation

| | |
|---|---|
| $a$ | Scalar. |
| $\boldsymbol{a}$ | Vector. |
| $\boldsymbol{A}$ | Matrix. |
| $\boldsymbol{A}^{-1}$ | Inverse of the matrix $\boldsymbol{A}$. |
| $\boldsymbol{A}^{\dagger}$ | Pseudo-inverse of the matrix $\boldsymbol{A}$. |
| $\boldsymbol{A}^{T}$ | Transpose of a matrix. |
| $\boldsymbol{A}^{*}$ | Complex conjugate of a matrix. |
| $\boldsymbol{A}^{H}$ | Transpose and complex conjugate of a matrix (Hermitian). |
| $\mathbf{0}$ | Vector/matrix of zeros of the appropriate dimensions. |
| $\boldsymbol{I}$ | Identity matrix of the appropriate dimensions. |
| $\mathrm{Tr}\,(\boldsymbol{A})$ | Trace of the matrix $\boldsymbol{A}$. |
| $\lvert\boldsymbol{A}\rvert$ | Determinant of the matrix $\boldsymbol{A}$. |
| $\mathrm{rank}\,(\boldsymbol{A})$ | Rank of the matrix $\boldsymbol{A}$. |
| $\ker(\boldsymbol{A})$ | Kernel/null-space of the matrix $\boldsymbol{A}$. |
| $\mathrm{blkdiag}\,(\boldsymbol{A}_1, \ldots, \boldsymbol{A}_N)$ | Block diagonal matrix formed with the matrices $\{\boldsymbol{A}_1, \ldots, \boldsymbol{A}_N\}$. |
| $\mathrm{diag}\,(a_1, \ldots, a_N)$ | Diagonal matrix whose main diagonal is $\{a_1, \ldots, a_N\}$. |
| $\mathrm{eig}\,(\boldsymbol{A})$ | Diagonal matrix whose main diagonal are the eigenvalues of the matrix $\boldsymbol{A}$. |
| $\lVert\boldsymbol{a}\rVert_2$ | Norm-2 (Euclidean norm) of the vector $\boldsymbol{a}$, see (3.49). |
| $\lVert\boldsymbol{A}\rVert_F$ | Frobenius norm of the matrix $\boldsymbol{A}$, see (**??**). |
| $\boldsymbol{\nabla}_{\boldsymbol{x}} f(\boldsymbol{x})$ | Gradient of a function $f(\boldsymbol{x})$, (3.53). |
| $\mathbb{E}\{\cdot\}$ | Statistical expectation. |

| | |
|---|---|
| $\log(\cdot)$ | Natural (base $e$) logarithm. |
| $\log_2(\cdot)$ | Base 2 logarithm. |
| $[a]^+$ | $\max(0, a)$. |
| $\mathbb{R}$ | Field of real numbers. |
| $\mathbb{R}^+$ | Set of positive real numbers. |
| $\mathbb{R}^+ \cup \{0\}$ | Set of non-negative real numbers. |
| $\mathbb{C}$ | Field of complex numbers. |

# Acronyms

**3G** $3^{rd}$ Generation of Mobile Communications.

**3GPP** $3^{rd}$ Generation Partnership Project.

**4G** $4^{th}$ Generation of Mobile Communications.

**5G** $5^{th}$ Generation of Mobile Communications.

**AWGN** Additive White Gaussian Noise.

**BC** Broadcast Channel.

**BD** Block Diagonalization.

**BIA** Blind Interference Alignment.

**BS** Base Station.

**CA** Carrier Aggregation.

**CDF** Cumulative Distribution Function.

**CoMP** Coordinated Multi Point.

**CSI** Channel State Information.

**DPC** Dirty Paper Coding.

**HetNet** Heterogeneous Networks.

**HSPA+** High-Speed Packet Access Plus.

**IA** Interference Alignment.

**iid** independent identically distributed.

**IMT-Advanced** International Mobile Telecommunications-Advanced.

**ITU-R** International Telecommunication Union Radiocommunication Sector.

**KKT** Karush-Kuhn-Tucker.

**LTE** Long Term Evolution.

**LTE-A** Long Term Evolution Advanced.

**MAC** Multiple Access Channel.

**MIMO** Multiple Input Multiple Output.

**MMSE** Minimum Mean Squared Error.

**MSE** Mean Squared Error.

**MU-MIMO** Multi User Multiple Input Multiple Output.

**OCI** Other Cluster Interference.

**OFDM** Orthogonal Frequency Division Multiplexing.

**OFDMA** Orthogonal Frequency Division Multiple Access.

**PAPC** Per Antenna Power Constraint.

**PBPC** Per Base Station Power Constraint.

**pdf** probability density function.

**RN** Relay Node.

**SINR** Signal to Interference plus Noise Ratio.

**SISO** Single Input Single Output.

**SNR** Signal to Noise Ratio.

**SU** Single User.

**SVD** Singular Value Decomposition.

**TPC** Total Power Constraint.

**UFR** Universal Frequency Reuse.

**WCDMA** Wide-band Code Division Multiple Access.

**ZF** Zero Forcing.

# Chapter 1

# Introduction

Every new generation of cellular network technologies comes with a new set of requirements, dictated by the trends in the use of the mobile connectivity. One common requirement in every generation is to obtain higher data rates and greater power efficiency. The requirement motivates research and technology innovation in order to achieve the goals set for each generation.

The research associated usually requires revisiting old paradigms used in previous generations, and updating them with novel ideas.

*Release 7* of the $3^{rd}$ Generation Partnership Project (3GPP) $3^{rd}$ Generation of Mobile Communications (3G) specifications [4], also known as High-Speed Packet Access Plus (HSPA+), included the use of MIMO as a means to increase the transmission rates.

*Release 8*, more well known by its commercial name Long Term Evolution (LTE) [2], introduced a new physical layer, based on Orthogonal Frequency Division Multiplexing (OFDM) instead of Wide-band Code Division Multiple Access (WCDMA) as in 3G. Although the rates attainable with WCDMA may be comparable to those obtained with OFDM, the latter provides a much easier equalization mechanism that makes dealing with multipath channels a simpler task. Apart from that, OFDM provides a higher flexibility in the resource allocation and enables the use of Orthogonal Frequency Division Multiple Access (OFDMA).

However, LTE did not meet the requirements issued by the International Telecommunication Union Radiocommunication Sector (ITU-R) International Mobile Telecommunications-Advanced (IMT-Advanced) radio interface [45] for what is known as $4^{th}$ Generation of Mobile Communications (4G).

The introduction of Long Term Evolution Advanced (LTE-A) in *release 10* of the LTE specification [3] met the requirements to be considered an IMT-Advanced system.

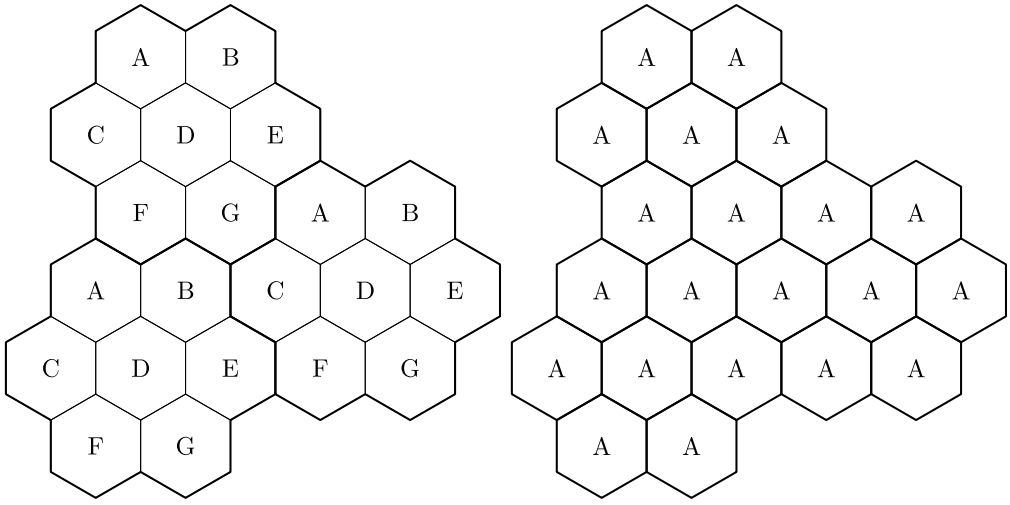


(a) Frequency reuse factor of 1/7. (b) Frequency reuse factor of 1.

Figure 1.1: Different frequency planning options

The main novelties included in LTE-A are Carrier Aggregation (CA), enhanced use of MIMO techniques and support for Relay Nodes (RNs).

*Release 11* [1] included in its specification the support for Coordinated Multi Point (CoMP) operation. CoMP was considered in order to improve the network performance at cell edges, for it uses several transmitters to provide coordinated transmission in the downlink, and a number of receivers to provide coordinated reception in the uplink.

With LTE-A standardized and its deployment already ongoing, further releases of LTE-A still continue but standards bodies and industry are already looking to the future $5^{th}$ Generation of Mobile Communications (5G), as is doing the research world. Even though there is no definite idea about what 5G will be, it is clear what it will *not* be: an incremental advance on 4G. It needs to be a paradigm shift [5].

The new 5G systems will be characterized by being heterogeneous, formally known as Heterogeneous Networkss (HetNets), formed by multiple small cells, using different radio access technologies [20]. One of the main problems for HetNets is inter-cell interference, because of the possible presence of unplanned deployment of small cells, and the irregular shape of the cells. Hence the importance of interference coordination techniques.

Current MIMO systems used in cellular networks are not achieving the expected performance predicted by the initial theoretical works. The main reason for this is the interference that is present naturally in cellular systems when all cells share the same spectrum for the tranmissions. The effect of this interference is a reduction of the Signal to Interference plus Noise Ratio (SINR) experienced by the users, highly reducing the advantages that MIMO could potentially deliver.

The conventional approach for cellular networks was to carefully plan the allocation

of frequencies in order to avoid the interference among neighboring cells. Clusters of $N$ cells were grouped together, and assigned $N$ frequency bands to be used, and the pattern is repeated for different clusters, yielding what is called a *frequency reuse factor* of $1/N$, as exemplified in Figure 1.1a.

The problem that this poses is that the available spectrum must be split, which is an inherent inefficiency in the use of the resources.

A different option consists of a system where all the cells share a common spectrum, so that all of them can use the full amount of resources available. This is called UFR, and a graphical description can be seen in Figure 1.1b.

It is in this kind of network that the need for coordination among cells arises, as every cell will interfere with the rest of the cells in the system, reducing the SINR operating point of the users.

In the search for higher data rates and a more efficient use of the resources, UFR is needed make the most out of the scarce radio frequency spectrum. Therefore, "a new look at the interference" [31] is needed. The conventional concept of the interference as an impairment needs to shift to a new viewpoint where the interference can be used to improve the overall performance of the network. A joint optimization of the resources among all the cells is required in order to globally improve the perfomance of the system [30].

The CoMP operation considered in [1] is just a part of a much broader field of multicell cooperation or coordinated communications where several cells are assumed to cooperate, in the sense that they take measures to alleviate the level of interference introduced into other parts of the network to a certain degree, or the use of that interference to their advantage.

Intuitively, the best strategy should be to allow all the BSs in the network to cooperate, in what is known as *global coordination*. Even though it may seem that global coordination could solve all the problems of frequency planning and resource allocation, it cannot be ignored that it comes at a non-negligible cost. The BSs in the network may need to interchange information in order to cooperatively transmit the data to all the users in the system. The amount of information that needs to be exchanged becomes unmanageable with the size of the network, i.e., the number of BSs that form the system. The result of this is that the capacity required to transmit this information renders the alleged solution useless. Not only are the backhaul transmission capabilities required prohibitive, but also tight synchronization among the BSs becomes a challenge, and channel information gathering becomes a cumbersome task. Apart from this, theoretical works [62] have unveiled intrinsic limitations of cooperation, whose benefits do not unboundedly grow with the size of the coordination group.

For all these reasons, clustering appears as a means to cope with the limitations of global coordination. In clustering, the coordination is not performed among all

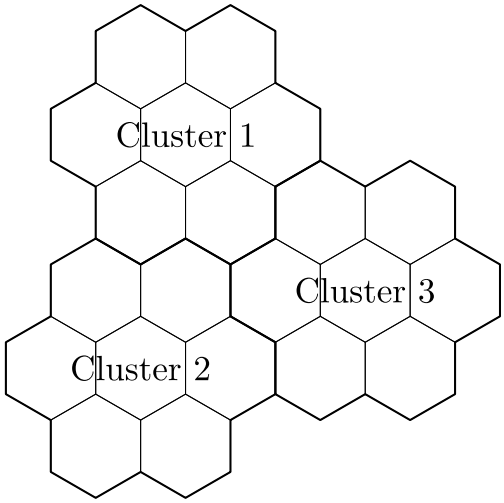


Figure 1.2: Clustered network scenario.

the BSs in the network but, instead, small groups, or clusters, are formed and the cooperation takes place locally within the cluster. This greatly reduces the amount of control information that should be handled by the backhaul. Also, the reduced size of the group makes the system work at an operating point where the natural limitations mentioned in [62] do not affect the performance of the network.

A schematic representation of a clustered network can be seen in Figure 1.2 where three clusters of seven cells are shown.

Grouping the cells in reduced size clusters has an important drawback: if the cooperation is done within a cluster and neighboring clusters are not coordinated in any way, there would be, again, unhandled interference, albeit not the same as in the uncoordinated scenario.

This thesis focuses on a clustered cellular network where BD is used for coordination within each cluster. The performance of the network, in terms of achievable rate and fairness considerations, is analyzed, and its dependence on several parameters of the network is studied. Also, mechanisms to deal with the interference, resulting from clustering, are presented.

The main contributions of this thesis are:

- Roberto Corvaja, Juan José García Fernández, and Ana García Armada. "Mean Achievable Rates in Clustered Coordinated Base Station Transmission With Block Diagonalization". In: *IEEE Transactions on Communications* 61.8 (Aug. 2013), pp. 3483–3493
- Roberto Corvaja, Juan José García Fernández, and Ana García Armada. "Achievable Rate and Fairness in Coordinated Base Station Transmission". In: *Communications Letters, IEEE* 18.4 (Apr. 2014), pp. 584–587

- Juan José García Fernández et al. "Adaptive Block Diagonalization and User Scheduling With Out of Cluster Interference". In: *European Wireless 2014; 20th European Wireless Conference; Proceedings of*. May 2014, pp. 1–6

The organization of the present document is as follows:

- In Chapter 2 a compilation of different alternatives for coordination, as well as for clustering, found in the literature are presented and described.
- Chapter 3 presents the system model used throughout the dissertation, and describes in detail BD and the power allocation strategies used in the rest of the work.
- Chapter 4 analyzes the performance of a cellular network, in terms of the mean achievable rate as a function of the cluster size, when using BD for coordination within each cluster, and taking into account the interference due to external clusters. An analytical expression for the mean achievable rate is developed and the optimum cluster size is obtained.
- Chapter **??** considers the fairness of the system, and studies the variability of the rate, as a complement to the mean obtained in Chapter 4. The behavior of the rates is shown to follow almost exactly a Gamma distribution.
- The pernicious effect of the OCI in the rates is introduced in Chapter **??**, and a mechanism to deal with it, based on a mixed transmission strategy and on a scheduling algorithm, is presented.
- Finally, some concluding remarks and future research lines are discussed in Chapter **??**.

# Chapter 2

# Analysis of the State of the Art

This thesis deals with three main topics:

- Interference Management.
- Clustering.
- Scheduling.

This chapter presents a brief literature review on these fields, in order to put this thesis in perspective. Interference management represents the cornerstone of this document, hence it will be more thoroughly treated.

## 2.1 Interference management

The bulk of the work of this thesis is around interference management and, in particular, around BD, which is just a concrete case of a much broader field.

Interference management techniques can be organized according to the information requiered for the process to work:

- *Beamforming*: in order to perform beamforming, both Channel State Information (CSI) and user data should be shared among the transmitters. BD lies within this category.
- *Interference Alignment*: user data is not required for interference alignment to work, but CSI is still needed.
- *Blind techniques*: finally there are theoretical alternatives which may enable the interference management without *a priori* knowledge about CSI or user data.

### 2.1.1 Beamforming

Most of the work about beamforming applied to cellular networks was initially based on the adaptation of Multi User Multiple Input Multiple Output (MU-MIMO) processing techniques to the context of multi-cell cooperation, [31].

In particular the Broadcast Channel (BC) and Multiple Access Channel (MAC) are of special interest, because a coordinated cellular network closely resembles these two channels, on the downlink and on the uplink respectively. In [17] the achievable rate region of the MIMO BC is analyzed for the case of single antenna receivers, and it is shown that the use of Dirty Paper Coding (DPC) is required to achieve such region. The scenario with multiple antenna receivers is studied in [95], using the same strategy based on DPC.

While these works studied the achievable rate region using a given strategy, the actual capacity for the BC was calculated in [94] and extended in [90]. This capacity was also calculated using the so called MAC-BC duality which was presented [52] for the Single Input Single Output (SISO) case, and in [89] and [51] for the multiple antenna scenario.

This thesis focuses on BD, which was introduced in [82] which, in turn, has spawned extensive research [83, 93, 32, 77, 91, 84], just to name a few. BD was originally formulated for MU-MIMO, but as with other techniques, it has also been used for cooperative cellular networks. In general, BD is inferior in terms of sum capacity to DPC. Nevertheless, in the special case where BD is combined with the right user selection algorithms, BD can come close to the sum capacity of DPC [93], [77]. .

The existing results for the MAC apply directly to a multicell setup [49]. Despite the MAC-BC duality, the extension of MIMO BC results to the multicell world presents several problems, being one of the most important the power constraints. In the case of a traditional MIMO BC, the multiple antennas are collocated at a single transmitter and, therefore, the power constraint is only one (arguably, this is not completely true, because the power used for the transmission may not be shared among antennas) while for the multicell case, the different transmitters do not share a power constraint, yielding a whole different problem formulation.

Early approaches like [76] and [75] dealt with a cellular downlink as if it were a classical BC, from the information theoretical point of view. The key for their analysis is the use of the rather unrealistic assumption of a sum-power constraint. They also share the single antenna transmitters and receivers scenario formulation, and they differ in the objective function that is considered, sum-rate [76] and individual SINR constraints per user in [75]. A similar scheme to [76] and [75] is used in [54], with a linear precoder based on the LQ factorization together with DPC to handle the remaining interference. The main difference in this work is that they consider a MIMO scenario and, more

importantly, the power constraint is set per base station, which is a much more realistic assumption.

In [88] they propose the study of a realistic scenario in order to analyze the advantages of "Network MIMO" when moderately realistic assumptions are considered. The more realistic system model can be tackled because they consider the uplink, where the assumptions needed to apply conventional MIMO MAC strategies are simpler than for the downlink.

A first approach to using BD in a multi-cell setup can be found in [80], where no actual coordination exists among the different cells, but they independently use BD to serve their users. The key of this work is that they consider a strategy that takes into account the interference coming from other cells, in the form of the interference plus noise covariance matrix. [96] goes one step further, by considering per-base-station power constraint, and by considering clusters of coordinated BS and partial coordination among clusters. It also introduces a novel power allocation scheme, *scaled water-filling* which is used in this thesis for its simplicity and good performance, despite being suboptimal. The per-base-station power constraint is also considered in [97], [60], [10].

In [80] they already proposed the use of limited size clusters, in order to alleviate the burden put unto the backhaul network, feedback channels and processing capabilities. But not only the complexity of the joint processing increases with the size of the network, but research also shows that there may be other limiting factors to the gains that can be achieved through coordination [62], [7]. The first problem, the complexity increase, can be handled by avoiding CSI sharing and through distributed cooperation [85], [8], [44], [12], [39]. Another approach to deal with that problem is reducing the number of cells that are coordinated, what is called as clustering. The research on this topic will be reviewed in Section 2.2.

It is worth noting, albeit not studied within this thesis, that other linear schemes based on minimizing the Mean Squared Error (MSE) have also been proposed, yielding different precoding matrices [79], [63], [28], [78], [11], [81].

### 2.1.2 Interference Alignment

The idea behind Interference Alignment (IA) is to find a way of restricting the interference subspace to lie within a small subspace that does not span the entire signal space at the receiver. This way, the desired signals can be projected into the null space of the interference and, by that means, recovered free from interference. The advantage of this is that, even though CSI is still required to achieve that, there is no need to share user data, which is a big reduction in the amount of information that is exchanged among the transmitters.

An exhaustive survey on IA can be found in [47]. The initial works on this dealt with the MIMO X channel, with two users, [64], [50], and it was extended to support a bigger

number of users in the K user interference channel [16]. This in turn was extended to the case of a MIMO interference channel [34]. A variety of increasingly sophisticated forms have arised from these initial works, [48], [14], [58] among others.

In any case, IA has found little use in real world applications, and it remains as a very elegant and interesting theoretical field.

### 2.1.3 Blind techniques

A further refinement over IA is Blind Interference Alignment (BIA) [35], [46] and [67]. In this case the channel coefficients are not required in order to align the interference, and it is only needed to have information about the coherence time of the channel, for these methods rely on the use of a so-called supersymbol, during which the channel should stay unchanged. As with regular IA, the main drawback is the SNR regime required to perform as expected, which usually exceeds the operation levels of real world cellular networks.

## 2.2 Clustering

As it has been said in Chapter 1, coordinating all the BSs in the system has drawbacks that can be alleviated reducing the number of elements that coordinate. This can be achieved using clustering as a means to group a reduced number of BSs that will cooperatively process and transmit information to the users.

Clustering can be done in several ways, and the particular characteristics of an actual cluster formation may be highly dependent on the specific scenario to be considered.

For analysis purposes the types of clusters can be grouped according to the actual layout of the clusters, whether a given transmitter is allowed to belong to more than one cluster at the same time or not:

- Non-overlapping.
- Overlapping.

An alternative, non-exclusive characterization depends on the dynamic nature of the clusters, whether they change over time or they stay fixed once they are set:

- Fixed.
- Dynamic.

In general, to make a certain clustering arrangement, it is necessary a metric, a criterion to group several BSs. Here there is a wide variety of choices in the literature:

- Proximity of the BSs.
- SNR of the link to each BS.
- Level of interference coming from each BS.
- Orthogonality of the channels.
- Transmission strategy design.
- Heuristic approaches.

The most common option, and simplest, is to have disjoint clusters, formed by proximity of the BSs, and fixed in time. The main advantage of this setup is, precisely, its simplicity. Fixed clusters over time avoid the need for reconfiguration, and the need for control information to be exchanged in order to update the clusters configuration. This is the main reason why this is the option used in this thesis. But it can also be found in many other references [96], [43], [74], [42]. This advantage comes, in fact, from the fixed nature of the clusters, and not necessarily from the distance metric, or the non-overlapping organization. In [86], fixed, non-overlapping clusters are also proposed, but the metric used to build the clusters is more sophisticated. They select the BSs that have orthogonal channels to the users, which is advantageous when Zero Forcing (ZF) is used for coordination within each cluster.

The other alternative is to have dynamic clusters, whose configuration may change in time, evolving to meet the changing nature of the channel. The most natural way of having dynamic clusters is when these groups of cells are user-centric, i.e., the clusters are formed around each user. If the user moves, by definition, the clusters will vary accordingly. Another characteristic of user-centric clusters is that they are overlapping. [68] is an example of such a system, where the BSs that coordinate to transmit to each user are assigned using a user-centric metric. In this case two different metrics are proposed: distance based, and level of interference, intuitively it is more likely to get a higher gain if the most interfering BSs are coordinated. A similar approach is used in [33], with overlapping, user-centric clusters of fixed size, or of variable size according to the relative signal strength received from each BS.

An interesting combination can be found in [6], where user-centric clusters are used, but where the resulting clusters are disjoint. The way to achieve this is by carefully selecting which users are served simultaneously.

On the other hand, there may be dynamic clusters which are not user-centric. This is the case of [70], [69], [71], [65], [26], [57], and [41]. In general these approaches have in common that the clustering is the by-product of another process, such as an optimization problem to reduce the amount of feedback needed [71], [57], or the heuristic metrics used in [65].

In general, dynamic, overlapping clusters have the main drawback of requiring a more complex management, needing a higher amount of control information to set them up and to update them.

## 2.3 Scheduling

In general, multi-user techniques can deal with just so many users in the system so that, when the number of users is too high, scheduling is required to ensure that all users are served, in order to keep the fairness of the system controlled. In [93], the users are selected according to the mutual orthogonality, and they combine it with a classical round robin scheduling, which guarantees a maximum delay, and with a proportional fair strategy, which enforces more strongly the fairness at the expense of not guaranteeing the maximum delay in the transmissions. In [66], a heuristic algorithm is proposed in order to successively schedule the users, in order to enforce fairness.

A similar, yet different use can be found in [70] and [55] where a dynamic scheduling algorithm is used in order to improve the fairness of the system, by reducing the effect of the edge users in the performance of the network.

More sophisticated scheduling alternatives have been studied in [92] and [56], with essentially the same objective of controlling the equity of the system.

While most of the scheduling research relies on finding an equitable solution for the users transmission, a different use is proposed in [6], where the user scheduling is a tool in order to enforce the creation of disjoint clusters, easing like that the management of such a clustered network.

# Chapter 3

# System Model

## 3.1 System Model

The system that will be considered throughout this work aims to represent the downlink of a canonical cellular network, comprising several identical cells, laid out over a regular hexagonal grid.

When studying a cellular network, the cells located at the edge of the network will not experience the same conditions as the cells in the center of the network. A typical way to deal with this situation is to consider a scenario that wraps around (Figure 3.2a) so that cells on one side of the scenario affect cells on the opposite side. Another option is to consider a scenario with more cells than necessary, and then analyze the behavior of the cells located within the center of the network (Figure 3.2b), so that the exterior cells account for the interference, equaling the conditions of all the cells in the network.

Each cell in the system under study will be served with a single BS that is equipped with $t$ transmit antennas. Each of the users considered in the system has $r$ receive antennas. Figure 3.1 shows a schematic representation of such a network, where $R_{\text{cell}}$ is the cell radius, and $d_{ij}$ is the distance from the $j$-th BS to the $i$-th user. Each user is supposed to be associated with a single BS and, without loss of generality, it is assumed that the $i$-th user is served by the $i$-th BS, and in the following the distance between a user and its serving BS will be denoted by $d_i \triangleq d_{ii}$.

A system with $M$ BSs and $N$ users can then be modelled as

$$\boldsymbol{y} = \boldsymbol{H}\boldsymbol{x} + \boldsymbol{n} \tag{3.1}$$

where $\boldsymbol{y}$ represents the signal received at all the users and is defined as

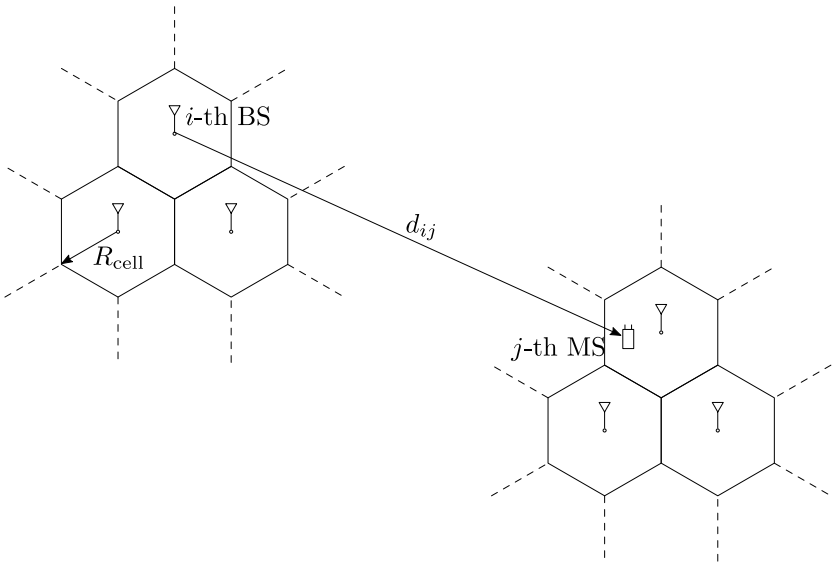


Figure 3.1: Schematic representation of the cellular network that will be used throughout this dissertation.

$$\boldsymbol{y} = \begin{bmatrix} \boldsymbol{y}_1 \\ \vdots \\ \boldsymbol{y}_N \end{bmatrix} \in \mathbb{C}^{Nr \times 1} \tag{3.2}$$

where $\boldsymbol{y}_i \in \mathbb{C}^{r \times 1}$ is the signal received at the $i$-th user.

$\boldsymbol{H}$ is the channel matrix representing the propagation from all the BSs to all the users, with the following structure

$$\boldsymbol{H} = \begin{bmatrix} \boldsymbol{H}_{11} & \cdots & \boldsymbol{H}_{1M} \\ \vdots & \ddots & \vdots \\ \boldsymbol{H}_{N1} & \cdots & \boldsymbol{H}_{NM} \end{bmatrix} \in \mathbb{C}^{Nr \times Mt} \tag{3.3}$$

where $\boldsymbol{H}_{ij} \in \mathbb{C}^{r \times t}$ represents the channel matrix from the $j$-th BS to the $i$-th user. It will include the path loss due to propagation, small scale fading, shadowing, and any other characteristic of the radio channel that needs to be taken into consideration.

The vector $\boldsymbol{x}$ in (3.2) is the signal transmitted from all the BSs, and it is composed of

$$\boldsymbol{x} = \begin{bmatrix} \boldsymbol{x}_1 \\ \vdots \\ \boldsymbol{x}_M \end{bmatrix} \in \mathbb{C}^{Mt \times 1} \tag{3.4}$$

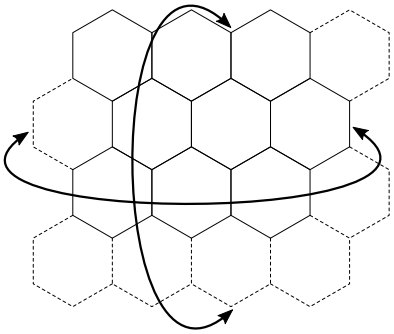

(a) Wrap around scenario. Cells on one side of the scenario influence the cells on the other side as if they were next to each other.

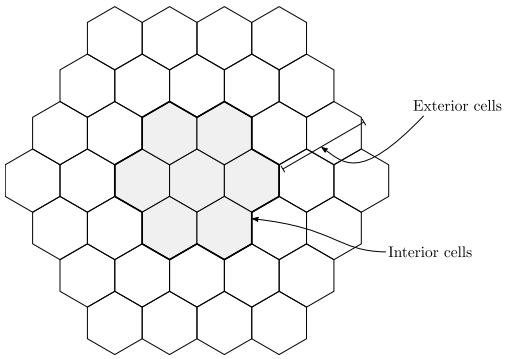


(b) Oversized scenario. The behavior of the network is analyzed in the central cells of the network, and the exterior cells compensate the network edge effects.

Figure 3.2: Different scenario configurations.

where $\boldsymbol{x}_j \in \mathbb{C}^{t\times 1}$ is the signal transmitted by the $j$-th BS. Additionally, the power transmitted by the $j$-th BS can be calculated from the transmitted signal as

$$P_{j,\mathrm{tx}} = \mathrm{Tr}\left(\boldsymbol{x}_j \boldsymbol{x}_j^H\right) = \boldsymbol{x}_j^H \boldsymbol{x}_j \tag{3.5}$$

and each BS will have an independent power constraint

$$P_{j,\mathrm{tx}} \leq P_{j,\mathbf{max}}. \tag{3.6}$$

Finally $\boldsymbol{n}$ represents the Additive White Gaussian Noise (AWGN) at all the receivers

$$\boldsymbol{n} = \begin{bmatrix} \boldsymbol{n}_1 \\ \vdots \\ \boldsymbol{n}_N \end{bmatrix} \in \mathbb{C}^{Nr\times 1} \tag{3.7}$$

with $\boldsymbol{n}_i \in \mathbb{C}^{r\times 1}$ accounts for the Gaussian noise at the $i$-th receiver. Throughout this work $\boldsymbol{n}_i$ is considered to be formed by independent identically distributed (iid) entries, drawn from a zero mean, $\sigma_i^2$ variance Gaussian distribution, $\boldsymbol{n}_i \sim \mathcal{N}\left(\boldsymbol{0}, \sigma_i^2 \boldsymbol{I}\right)$. The noise variance will be assumed the same for all the receivers.

In a general scenario, there may be cooperation among the BSs in the system so that the information intended for a particular user will be transmitted by several or all the BSs. Or, equivalently, each BS transmits a combination of the information of several users

$$\boldsymbol{x}_j = \boldsymbol{W}_{j1}^{(\mathrm{tx})}\boldsymbol{s}_1 + \cdots + \boldsymbol{W}_{jN}^{(\mathrm{tx})}\boldsymbol{s}_N \tag{3.8}$$

where $\boldsymbol{s}_i \in \mathbb{C}^{\ell \times 1}$ is the vector of information symbols to be transmitted to user $i$, with $\ell$ being the number of simultaneous symbols or streams to be transmitted to that user. $\boldsymbol{W}_{ji}^{(\mathrm{tx})} \in \mathbb{C}^{t \times \ell}$ is the precoding matrix used at the $j$-th transmitter for the data of the $i$-th user.

It will be assumed that the information symbols are independent and drawn from a Gaussian distribution such that $\boldsymbol{s}_i \sim \mathcal{N}\left(\boldsymbol{0}, \boldsymbol{R}_{\boldsymbol{s}_i}\right)$, where $\boldsymbol{R}_{\boldsymbol{s}_i} = \mathrm{diag}\left\{p_{i1}, \ldots, p_{i\ell}\right\} \in \mathbb{R}^{\ell \times \ell}$ contains the power allocated to each of the symbols in $\boldsymbol{s}_i$. The transmitted power can be expressed as

$$P_{j,\mathrm{tx}} = \sum_{i=1}^{N} \mathrm{Tr}\left(\boldsymbol{W}_{ji}^{(\mathrm{tx})} \boldsymbol{R}_{\boldsymbol{s}_i} \boldsymbol{W}_{ji}^{(\mathrm{tx}),H}\right). \tag{3.9}$$

The choice of the precoding matrices and of the receiving filter will determine the transmission strategy used. This thesis will focus mainly on BD [82] which is described in Section 3.3.

On the receiver side, no cooperation among the users will be considered, so each user may perform, independently, additional processing of the received signal by applying a linear filter or equalizer

$$\hat{\boldsymbol{s}}_i = \boldsymbol{W}_i^{(\mathrm{rx})} \boldsymbol{y}_i \tag{3.10}$$

where $\boldsymbol{W}_i^{(\mathrm{rx})} \in \mathbb{C}^{r \times \ell}$ is the equalizer used at the $i$-th receiver.

Combining (3.1)–(3.8) it is possible to rewrite (3.1) as

$$\boldsymbol{y} = \boldsymbol{H}\boldsymbol{W}^{(\mathrm{tx})}\boldsymbol{s} + \boldsymbol{n} \tag{3.11}$$

where

$$\boldsymbol{s} = \begin{bmatrix} \boldsymbol{s}_1 \\ \vdots \\ \boldsymbol{s}_N \end{bmatrix} \in \mathbb{C}^{N\ell \times 1} \tag{3.12}$$

and the global precoding matrix is

$$\boldsymbol{W}^{(\mathrm{tx})} = \begin{bmatrix} \boldsymbol{W}_{11}^{(\mathrm{tx})} & \cdots & \boldsymbol{W}_{1N}^{(\mathrm{tx})} \\ \vdots & \ddots & \vdots \\ \boldsymbol{W}_{M1}^{(\mathrm{tx})} & \cdots & \boldsymbol{W}_{MN}^{(\mathrm{tx})} \end{bmatrix} \in \mathbb{C}^{Mt \times N\ell} \tag{3.13}$$

and it can be partitioned as

$$\boldsymbol{W}^{(\mathrm{tx})} = \left[\boldsymbol{W}_1^{(\mathrm{tx})}, \ldots, \boldsymbol{W}_N^{(\mathrm{tx})}\right] \tag{3.14}$$

with

$$\boldsymbol{W}_i^{(\mathrm{tx})} = \begin{bmatrix} \boldsymbol{W}_{11}^{(\mathrm{tx})} \\ \vdots \\ \boldsymbol{W}_{M1}^{(\mathrm{tx})} \end{bmatrix} \in \mathbb{C}^{Mt \times \ell}. \tag{3.15}$$

The channel matrix can then be partitioned as

$$\boldsymbol{H} = \begin{bmatrix} \boldsymbol{H}_1 \\ \vdots \\ \boldsymbol{H}_N \end{bmatrix} \tag{3.16}$$

where $\boldsymbol{H}_i \in \mathbb{C}^{r \times Mt}$ is the channel matrix representing the propagation from all the BSs to the $i$-th user.

As it has already been mentioned, receiver cooperation is not going to be considered, so looking at a particular user, e.g., the $i$-th user, the signal that is received will be

$$\boldsymbol{y}_i = \boldsymbol{H}_i \boldsymbol{W}^{(\mathrm{tx})} \boldsymbol{s} + \boldsymbol{n}_i \tag{3.17}$$

which can be rewritten as

$$\boldsymbol{y}_i = \boldsymbol{H}_i \boldsymbol{W}_i^{(\mathrm{tx})} \boldsymbol{s}_i + \underbrace{\sum_{\substack{j=1 \\ j \neq i}}^{N} \boldsymbol{H}_i \boldsymbol{W}_j^{(\mathrm{tx})} \boldsymbol{s}_j}_{\text{Interference}} + \boldsymbol{n}_i \tag{3.18}$$

so that it can be readily seen how other users' data appear as an interference term that degrades the received signal.

Defining the term of interference plus noise as

$$\boldsymbol{z}_i = \sum_{\substack{j=1 \\ j\neq i}}^{N} \boldsymbol{H}_i \boldsymbol{W}_j^{(\mathrm{tx})} \boldsymbol{s}_j + \boldsymbol{n}_i \tag{3.19}$$

and using (3.18), the ergodic (mean) rate for the $i$-th user is given by [25], [40]

$$R_i = \mathbb{E}\left\{\log_2 \left| \boldsymbol{I} + \boldsymbol{H}_i \boldsymbol{W}_i^{(\mathrm{tx})} \boldsymbol{R}_{\boldsymbol{s}_i} \boldsymbol{W}_i^{(\mathrm{tx}),H} \boldsymbol{H}_i^H \boldsymbol{R}_{\boldsymbol{z}_i}^{-1} \right|\right\} \tag{3.20}$$

where $\boldsymbol{R}_{\boldsymbol{z}_i} \in \mathbb{C}^{r\times r}$ is the covariance matrix of the noise plus the interference term in (3.18)

$$\boldsymbol{R}_{\boldsymbol{z}_i} = \boldsymbol{z}_i \boldsymbol{z}_i^H = \left( \sum_{\substack{j=1 \\ j\neq i}}^{N} \boldsymbol{H}_i \boldsymbol{W}_j^{(\mathrm{tx})} + \boldsymbol{n}_i \right) \left( \sum_{\substack{j=1 \\ j\neq i}}^{N} \boldsymbol{H}_i \boldsymbol{W}_j^{(\mathrm{tx})} + \boldsymbol{n}_i \right)^H . \tag{3.21}$$

In the rest of the work, there are a set of assumptions that will be made, mainly to guarantee the feasibility of some of the results obtained:

- The number of users will be the same as the number of BSs, i.e., $N = M$.
- The total number of antennas transmitting will be greater or equal than the total number of antennas at the receiver side, this is $Mt \geq Nr$.
- The number of streams transmitted to each user must be $\ell \leq r$, and in general it will be assumed the equality.
- There is no correlation, neither at the transmitters nor at the receivers, so that $\boldsymbol{H}$ is full rank or, equivalently, $\mathrm{rank}\,(\boldsymbol{H}) = \min(Nr, Mt)$. As $Mt \geq Nr$, then $\mathrm{rank}\,(\boldsymbol{H}) = Nr$.
- The power available at each of the BSs will be assumed the same, i.e., $P_{j,\max} = P_{\max}$ for all $j$.

## 3.2 Channel Model

As it has been said, each component of $\boldsymbol{H}_{ij}$ accounts for the propagation path loss, small scale fading, shadowing, and other characteristics of the channel.

In terms of propagation, the channel is typically decomposed as

$$\boldsymbol{H}_{ij} = \boldsymbol{R}_{\mathrm{rx},ij} \boldsymbol{H}_{\mathrm{iid},ij} \boldsymbol{R}_{\mathrm{tx},ij} \tag{3.22}$$

where $\boldsymbol{R}_{\text{tx},ij} \in \mathbb{C}^{t\times t}$ is the spatial correlation at the transmitter, $\boldsymbol{H}_{\text{iid},ij} \in \mathbb{C}^{r\times t}$ is the uncorrelated fading channel, and $\boldsymbol{R}_{\text{rx},ij} \in \mathbb{C}^{r\times r}$ is the spatial correlation at the receiver. In the current work, unless stated otherwise, the channel is considered spatially uncorrelated, both at the transmitter and at the receiver, that is $\boldsymbol{R}_{\text{tx},ij} = \boldsymbol{I}$ and $\boldsymbol{R}_{\text{rx},ij} = \boldsymbol{I}$, as in [53].

The small scale characteristics considered are Rayleigh, so that the entries of $\boldsymbol{H}_{\text{iid},ij}$ are iid complex Gaussian random variables with zero mean and a variance given by the power path loss between the $j$-th BS and the $i$-th user.

The attenuation that the signal experiences due to the propagation varies according to an exponential power decay with exponent $\gamma$, so that the path loss* is calculated as

$$\text{pl}_{ij} = \text{pl}_0 \left(\frac{d_{ij}}{d_0}\right)^{-\gamma} \tag{3.24}$$

where $\text{pl}_0$ represents the attenuation at a reference distance $d_0$. For the analysis done in this work, but without any loss of generality, $\text{pl}_0$ and $d_0$ are assumed equal to 1.

### 3.2.1 SNR

With the definition of the propagation model that is used in this work, it can also be explained the definition of SNR that is used for the theoretical analyses and the simulations.

Analogously to other works such as [96], the SNR, denoted as $\rho$, is defined with reference to the power received at the three-way corner of the cell, at a distance of $R_{\text{cell}}$, when the BS transmits at full power, so that the relationship between SNR and the noise power is given by

$$\rho = \frac{P_{\max} R_{\text{cell}}^{-\gamma}}{\sigma_n^2} \tag{3.25}$$

where it is assumed that all the BSs have the same maximum transmission power. Using (3.25) it is possible to calculate the noise power for a given SNR and vice versa.

*In natural units, although it is also commont to represent the path loss in decibels as

$$\text{PL}_{ij}\,(\text{dB}) \triangleq 10\log_{10}\left(\text{pl}_{ij}\right) \tag{3.23}$$

## 3.3 Block Diagonalization

One possibility to cancel the inter-user interference is to diagonalize the channel matrix. Perfect diagonalization is only possible if $Mt \geq Nr$ [18], and it is achieved using the following precoding matrix

$$\boldsymbol{W}^{(\mathrm{tx})} = \boldsymbol{H}^{\dagger}. \tag{3.26}$$

This solution is optimum only when every user has only one antenna. In the case under study, with multiantenna receivers, complete diagonalization of the channel matrix is suboptimal since each user is able to coordinate the processing of its received signal.

In [82] is stated that the optimum solution under the constraint that all inter-user interference be zero is obtained with $\boldsymbol{H}\boldsymbol{W}^{(\mathrm{tx})}$ being block diagonal. In [82], BD is proposed as an algorithm to obtain a precoding matrix that is able to block diagonalize the channel matrix. This algorithm is described next.

In order to meet the condition of zero inter-user interference, it is necessary to cancel the interference term in (3.18), and this is equivalent to meet the following

$$\boldsymbol{H}_i \boldsymbol{W}_j^{(\mathrm{tx})} = \boldsymbol{0} \quad \forall j \neq i. \tag{3.27}$$

Let $\widetilde{\boldsymbol{H}}_i$ be the channel matrix $\boldsymbol{H}$ with the rows corresponding to the matrix $\boldsymbol{H}_i$ removed, i.e.,

$$\widetilde{\boldsymbol{H}}_i = \begin{bmatrix} \boldsymbol{H}_1 \\ \vdots \\ \boldsymbol{H}_{i-1} \\ \boldsymbol{H}_{i+1} \\ \vdots \\ \boldsymbol{H}_N \end{bmatrix} \in \mathbb{C}^{(N-1)r \times Mt}. \tag{3.28}$$

Then the condition (3.27) can be obtained making $\boldsymbol{W}_i^{(\mathrm{tx})}$ lie in the null space or kernel of $\widetilde{\boldsymbol{H}}_i$. This is possible only if the dimension of the null space is greater than zero, i.e., $\operatorname{rank}\left(\ker\left(\widetilde{\boldsymbol{H}}_i\right)\right) > 0$.

Now, with the dimensions of $\widetilde{\boldsymbol{H}}$, the rank of its null space is

$$\operatorname{rank}\left(\ker\left(\widetilde{\boldsymbol{H}}_i\right)\right) = Mt - \operatorname{rank}\left(\widetilde{\boldsymbol{H}}_i\right). \tag{3.29}$$

But it is assumed that $\boldsymbol{H}$ is full rank, ergo rank $\left(\widetilde{\boldsymbol{H}}_i\right) = (N-1)r = \widetilde{L}_i$, and then

$$\text{rank}\left(\ker\left(\widetilde{\boldsymbol{H}}_i\right)\right) = Mt - \widetilde{L}_i > 0 \tag{3.30}$$

so it is guaranteed that a precoding matrix $\boldsymbol{W}_i^{(\text{tx})}$ that lies in the null space of $\widetilde{\boldsymbol{H}}_i$ exists.

The simplest way to obtain such $\boldsymbol{W}_i^{(\text{tx})}$ involves using the Singular Value Decomposition (SVD) of the matrix $\widetilde{\boldsymbol{H}}_i$.

Let $\widetilde{\boldsymbol{H}}_i$ be decomposed as

$$\widetilde{\boldsymbol{H}}_i = \widetilde{\boldsymbol{U}}_i \widetilde{\boldsymbol{\Lambda}}_i \left[\widetilde{\boldsymbol{V}}_i^{(1)}, \widetilde{\boldsymbol{V}}_i^{(0)}\right]^H \tag{3.31}$$

where $\widetilde{\boldsymbol{V}}_i^{(0)} \in \mathbb{C}^{Mt \times (Mt - \widetilde{L}_i)}$ contains the last $Mt - \widetilde{L}_i$ right singular vectors of $\widetilde{\boldsymbol{H}}_i$, corresponding to the singular values equal to zero. $\widetilde{\boldsymbol{V}}_i^{(0)}$ forms an orthonormal basis of the null space of $\widetilde{\boldsymbol{H}}_i$, and thus its columns can be used to cancel the inter-user interference

$$\widetilde{\boldsymbol{H}}_i \widetilde{\boldsymbol{V}}_i^{(0)} = \boldsymbol{0}. \tag{3.32}$$

Using these matrices as precoding the result is

$$\widehat{\boldsymbol{H}} = \boldsymbol{H}\left[\widetilde{\boldsymbol{V}}_1^{(0)}, \ldots, \widetilde{\boldsymbol{V}}_N^{(0)}\right] = \begin{bmatrix} \boldsymbol{H}_1 \widetilde{\boldsymbol{V}}_1^{(0)} & & \boldsymbol{0} \\ & \ddots & \\ \boldsymbol{0} & & \boldsymbol{H}_N \widetilde{\boldsymbol{V}}_N^{(0)} \end{bmatrix} \tag{3.33}$$

that, as it can be seen, has a block diagonal structure, which gives the name to the algorithm proposed in [82].

The next problem that BD solves is the maximization of the sum-rate of the system, given the block diagonal structure in (3.33). The precoding matrix $\boldsymbol{W}_i^{(\text{tx})}$ will be considered to be

$$\boldsymbol{W}_i^{(\text{tx})} = \widetilde{\boldsymbol{V}}_i^{(0)} \boldsymbol{W}_i' \tag{3.34}$$

where $\boldsymbol{W}_i' \in \mathbb{C}^{(Mt - \widetilde{L}_i) \times \ell}$ will take care of the rate maximization.

Introducing (3.34) into (3.20) the ergodic capacity simplifies to

$$R_i^{\text{no interf}} = \mathbb{E}\left\{\log_2\left|\boldsymbol{I} + \frac{1}{\sigma_i^2}\widehat{\boldsymbol{H}}_i \boldsymbol{W}_i' \boldsymbol{R}_{\boldsymbol{s}_i} \boldsymbol{W}_i'^{,H} \widehat{\boldsymbol{H}}_i^H\right|\right\} \tag{3.35}$$

where $\widehat{\boldsymbol{H}}_i = \boldsymbol{H}_i \widetilde{\boldsymbol{V}}_i^{(0)} \in \mathbb{C}^{r\times(Mt-\widetilde{L}_i)}$.

In order to maximize the rate, consider the SVD

$$\widehat{\boldsymbol{H}}_i = \widehat{\boldsymbol{U}}_i \begin{bmatrix} \widehat{\boldsymbol{\Lambda}}_i & \boldsymbol{0} \\ \boldsymbol{0} & \boldsymbol{0} \end{bmatrix} \left[\widehat{\boldsymbol{V}}_i^{(1)}, \widehat{\boldsymbol{V}}_i^{(0)}\right]^H \tag{3.36}$$

where $\widehat{\boldsymbol{\Lambda}}_i = \text{diag}\left\{\hat{\lambda}_{i1}^{1/2}, \ldots, \hat{\lambda}_{ir}^{1/2}\right\} \in \mathbb{C}^{r\times r}$ contains the non-zero singular values of $\widehat{\boldsymbol{H}}_i$ , which has rank $\left(\widehat{\boldsymbol{H}}_i\right) = r$. And $\widehat{\boldsymbol{V}}_i^{(1)} \in \mathbb{C}^{(Mt-\widetilde{L}_i)\times r}$ contains the first $r$ right singular vectors of $\widehat{\boldsymbol{H}}_i$ , and it will be used as $\boldsymbol{W}_i'$, yielding the following precoding matrix

$$\boldsymbol{W}_i^{(\text{tx})} = \widetilde{\boldsymbol{V}}_i^{(0)} \widehat{\boldsymbol{V}}_i^{(1)} \tag{3.37}$$

The BD also provides the receiver filter to be used at each user which will be

$$\boldsymbol{W}_i^{(\text{rx})} = \widehat{\boldsymbol{U}}_i^H \tag{3.38}$$

Using all of the above, the rate that the $i$-th user can obtain is given by the expression

$$R_i^{\text{BD}} = \mathbb{E}\left\{\sum_{k=1}^{\ell} \log_2\left(1 + \frac{\hat{\lambda}_{ik} p_{ik}}{\sigma_i^2}\right)\right\} \tag{3.39}$$

where the only parameters left to be computed are the power allocated to each of the $\ell$ streams of each user, and different options to do it will be discussed in Section 3.4.

## 3.4 Power Allocation

In Section 3.3, the BD algorithm has been described to get the precoding matrix to be used at the transmitter and the equalization filter to be used at the receiver side. After BD has been used, the power should be allocated to each of the data streams of each user, this is, the $p_{ij}$ in (3.39) should be calculated in order to achieve a given performance, and subject to particular constraints.

The need for a power allocation algorithm comes from the restriction on the maximum power available for transmission, which may be due to physical limitations, or regulatory issues.

There are several different power constraints:

- Per Antenna Power Constraint (PAPC): The maximum power is constrained for each antenna at the transmitter. This option is specially well suited for distributed antenna systems [21], [59].
- Per Base Station Power Constraint (PBPC): In this case the maximum power is limited per base station instead of per antenna. This option is more appropriate for scenarios where all the transmitting antennas are collocated and may share a power budget, so that the transmission power can be arbitrarily allocated to each of the transmitter antennas.
- Total Power Constraint (TPC): it assumes that the maximum power is shared among all the transmitters in the system. Although this system is more easily analyzed, it is very unrealistic so it will not be considered in this work, except in Subsection 3.4.3 where a TPC is used to obtain an intermediate result.

For the sake of simplicity, PBPC will be used for the different analyses. In any case, PAPC can be seen as a particularization of PBPC as the derivations shown in this section can be applied to a PAPC system considering instead of each BS to have $t$ transmit antennas, $t$ single antenna BSs.

The problem that needs to be solved is, in general, the maximization of some function of the rate of each of the users subject to a PBPC

$$\begin{aligned} \underset{\{\boldsymbol{R}_{\boldsymbol{s}_i}\}}{\text{maximize}} \quad & f\left(R_i^{\mathrm{BD}}\left(\boldsymbol{R}_{\boldsymbol{s}_1},\right),\ldots,R_N^{\mathrm{BD}}\left(\boldsymbol{R}_{\boldsymbol{s}_N}\right)\right) \\ \text{subject to} \quad & P_{j,\mathrm{tx}} \leq P_{j,\mathrm{max}}, \quad j=1,\ldots,M \end{aligned} \tag{3.40}$$

One common metric used for the maximization is the weighted sum-rate of the system, so that the function $f(\cdot)$ is equal to

$$f\left(R_i^{\mathrm{BD}},\ldots,R_N^{\mathrm{BD}}\right)=\sum_{i=1}^{N}\alpha_i R_i^{\mathrm{BD}} \tag{3.41}$$

where $\alpha_i \in [0,1]$ can be seen as different priorities for different users, and they are assumed to be

$$\sum_{i=1}^{N}\alpha_i = 1 \tag{3.42}$$

and in the particular case where all the $\alpha_i = 1/N$, then the function $f(\cdot)$ represents the sum-rate of the system.

Calling

$$\overline{\boldsymbol{W}}_j^{(\mathrm{tx})} = \left[\boldsymbol{W}_{j1}^{(\mathrm{tx})}, \dots, \boldsymbol{W}_{jN}^{(\mathrm{tx})}\right] \in \mathbb{C}^{t \times N\ell} \tag{3.43}$$

the precoding matrix of the $j$-th BS, and

$$\boldsymbol{R}_{\boldsymbol{s}} = \mathrm{blkdiag}\left(\boldsymbol{R}_{\boldsymbol{s}_1}, \dots, \boldsymbol{R}_{\boldsymbol{s}_N}\right) \in \mathbb{C}^{N\ell \times N\ell} \tag{3.44}$$

the matrix containing the power assigned to all the streams of all the users, the power constraint in (3.40) can then be reformulated as

$$\mathrm{Tr}\left(\overline{\boldsymbol{W}}_j^{(\mathrm{tx})} \boldsymbol{R}_{\boldsymbol{s}} \overline{\boldsymbol{W}}_j^{(\mathrm{tx}),H}\right) \leq P_{j,\max} \tag{3.45}$$

Now the term inside the trace operator can be written explicitly as a function of $p_{ik}$ in order to make it easier to analyze. First define

$$\overline{\boldsymbol{W}}_j^{(\mathrm{tx})} = \left[\bar{\boldsymbol{w}}_{j,11}, \dots, \bar{\boldsymbol{w}}_{j,1\ell}, \dots, \bar{\boldsymbol{w}}_{j,N\ell}\right] \tag{3.46}$$

where $\bar{\boldsymbol{w}}_{j,ik} \in \mathbb{C}^{t \times 1}$ is the $ik$-th column of $\overline{\boldsymbol{W}}_j^{(\mathrm{tx})}$, i.e., the precoding that is used at the $j$-th BS for the $k$-th stream of the $i$-th user. And then:

$$\begin{aligned}
\overline{\boldsymbol{W}}_j^{(\mathrm{tx})} \boldsymbol{R}_{\boldsymbol{s}} \overline{\boldsymbol{W}}_j^{(\mathrm{tx}),H} &= \left[\bar{\boldsymbol{w}}_{j,11}, \dots, \bar{\boldsymbol{w}}_{j,N\ell}\right] \begin{bmatrix} p_{11} & & 0 \\ & \ddots & \\ 0 & & p_{N\ell} \end{bmatrix} \begin{bmatrix} \bar{\boldsymbol{w}}_{j,11}^H \\ \vdots \\ \bar{\boldsymbol{w}}_{j,N\ell}^H \end{bmatrix} = \\
&= p_{11} \bar{\boldsymbol{w}}_{j,11} \bar{\boldsymbol{w}}_{j,11}^H + \cdots + p_{N\ell} \bar{\boldsymbol{w}}_{j,N\ell} \bar{\boldsymbol{w}}_{j,N\ell}^H \\
&= \sum_{i=1}^{N} \sum_{k=1}^{\ell} p_{ik} \bar{\boldsymbol{w}}_{j,ik} \bar{\boldsymbol{w}}_{j,ik}^H
\end{aligned} \tag{3.47}$$

and the trace is

$$\mathrm{Tr}\left(\overline{\boldsymbol{W}}_j^{(\mathrm{tx})} \boldsymbol{R}_{\boldsymbol{s}} \overline{\boldsymbol{W}}_j^{(\mathrm{tx}),H}\right) = \sum_{i=1}^{N} \sum_{k=1}^{\ell} p_{ik} \left\|\bar{\boldsymbol{w}}_{j,ik}\right\|_2^2 \tag{3.48}$$

where

$$\left\|\bar{\boldsymbol{w}}_{j,ik}\right\|_2^2 = \mathrm{Tr}\left(\bar{\boldsymbol{w}}_{j,ik}\bar{\boldsymbol{w}}_{j,ik}^H\right) = \bar{\boldsymbol{w}}_{j,ik}^H\bar{\boldsymbol{w}}_{j,ik}. \tag{3.49}$$

The sum-rate maximization problem can then be formulated in *standard form* [13] as

$$\begin{aligned} \underset{p_{ik}}{\text{minimize}} \quad & -\sum_{i=1}^{N}\sum_{k=1}^{\ell}\log_2\left(1+\frac{\hat{\lambda}_{ik}p_{ik}}{\sigma_i^2}\right) & & \\ \text{subject to} \quad & \sum_{i=1}^{N}\sum_{k=1}^{\ell} p_{ik}\left\|\bar{\boldsymbol{w}}_{j,ik}\right\|_2^2 - P_{j,\max} \leq 0, & & j=1,\dots,M \\ & -p_{ik} \leq 0, & & \begin{array}{l} i=1,\dots,N \\ k=1,\dots,\ell \end{array} \end{aligned} \tag{3.50}$$

In the next sections, different alternatives for obtaining these powers are presented and described.

### 3.4.1 Optimal Power Allocation

In (3.50), the function $\log_2(\cdot)$ is convex on $p_{ik}$ and the sum of convex functions is also convex, so the objective function in (3.50) is convex. The constraints are affine and therefore convex too. The optimization problem in (3.50) is a convex optimization problem that can be solved using a different numerical techniques [13]. Nonetheless, it would be interesting to analyze a bit further the problem in order to get some insight about it.

The problem in (3.50) satisfies *Slater's condition* [13] since the objective function is convex and all the inequality constraints are affine, hence *strong duality* holds. This means that the optimum value of the primal problem is equal to the optimum value of the *Lagrange dual problem*, so that this can be used to find out the solution to the primal, original, problem.

Under these conditions, and considering that the objective function is differentiable with respect to $p_{ik}$, Karush-Kuhn-Tucker (KKT) conditions [13] are necessary and sufficient for optimality of a solution, and they can be used to analyze the optimization problem in search for an optimal solution. The KKT conditions for (3.50) are

$$
\begin{aligned}
\sum_{i=1}^{N}\sum_{k=1}^{\ell} p_{ik}^{*}\left\|\bar{\boldsymbol{w}}_{j,ik}\right\|_2^2 - P_{j,\max} &\leq 0, \quad j=1,\dots,M \\
p_{ik}^{*} &\leq 0, \quad \begin{matrix} i=1,\dots,N \\ k=1,\dots,\ell \end{matrix} \\
\nu_j^{*} &\geq 0, \quad j=1,\dots,M \\
\mu_{ik}^{*} &\geq 0, \quad \begin{matrix} i=1,\dots,N \\ k=1,\dots,\ell \end{matrix} \\
\nu_j^{*}\left(\sum_{i=1}^{N}\sum_{k=1}^{\ell} p_{ik}\left\|\bar{\boldsymbol{w}}_{j,ik}\right\|_2^2 - P_{j,\max}\right) &= 0, \quad j=1,\dots,M \\
-\mu_{ik}^{*}p_{ik}^{*} &= 0, \quad \begin{matrix} i=1,\dots,N \\ k=1,\dots,\ell \end{matrix} \\
\boldsymbol{\nabla}_{\boldsymbol{p}}\mathcal{L}\left(\boldsymbol{p}^{*},\boldsymbol{\nu}^{*},\boldsymbol{\mu}^{*}\right) &= \mathbf{0}
\end{aligned}
\tag{3.51}
$$

where the superscript $^*$ represents a feasible solution of the optimization problem, $\boldsymbol{\nabla}_{\boldsymbol{p}}$ is the gradient with respect to the powers $\boldsymbol{p} = [p_{11},\dots,p_{N\ell}]^T$, $\boldsymbol{\nu} = [\nu_1,\dots,\nu_M]^T$ and $\boldsymbol{\mu} = [\mu_{11},\dots,\mu_{N\ell}]^T$ are the Lagrange multipliers, and $\mathcal{L}$ represents the *Lagrangian* associated with the problem (3.50), and it is defined as

$$
\begin{aligned}
\mathcal{L}\left(\boldsymbol{p},\boldsymbol{\nu},\boldsymbol{\mu}\right) = &-\sum_{i=1}^{N}\sum_{k=1}^{\ell}\log_2\left(1+\frac{\hat{\lambda}_{ik}p_{ik}}{\sigma_i^2}\right) + \\
&\sum_{j=1}^{M}\nu_j\left(\sum_{i=1}^{N}\sum_{k=1}^{\ell}p_{ik}\left\|\bar{\boldsymbol{w}}_{j,ik}\right\|_2^2 - P_{j,\max}\right) - \\
&\sum_{i=1}^{N}\sum_{k=1}^{\ell}\mu_{ik}p_{ik}
\end{aligned}
\tag{3.52}
$$

The gradient of a function $f(\boldsymbol{x})$ with respect to $\boldsymbol{x}\in\mathbb{C}^{n\times 1}$ is defined as

$$
\boldsymbol{\nabla}_{\boldsymbol{x}} f(\boldsymbol{x}) = \begin{bmatrix} \frac{\partial}{\partial x_1} f(\boldsymbol{x}) \\ \vdots \\ \frac{\partial}{\partial x_n} f(\boldsymbol{x}) \end{bmatrix}
\tag{3.53}
$$

First the gradient of the objective function is calculated, by computing the partial derivatives

$$
\frac{\partial}{\partial p_{ik}}\left\{-\sum_{i=1}^{N}\sum_{k=1}^{\ell}\log_2\left(1+\frac{\hat{\lambda}_{ik}p_{ik}}{\sigma_i^2}\right)\right\} = \frac{-\hat{\lambda}_{ik}}{\log(2)\left(\sigma_i^2+\hat{\lambda}_{ik}p_{ik}\right)}
\tag{3.54}
$$

And the same for the inequality constraints

$$\begin{aligned} &\frac{\partial}{\partial p_{ik}} \left\{ \sum_{i=1}^{N} \sum_{k=1}^{\ell} p_{ik} \left\| \bar{\boldsymbol{w}}_{j,ik} \right\|_2^2 - P_{j,\max} \right\} = \left\| \bar{\boldsymbol{w}}_{j,ik} \right\|_2^2 \\ &\frac{\partial}{\partial p_{ik}} \{p_{ik}\} = 1 \end{aligned} \tag{3.55}$$

So that the condition of the gradient of the Lagrangian vanishing, in (3.50) can be writen as

$$\frac{-\hat{\lambda}_{ik}}{\log(2)\left(\sigma_i^2 + \hat{\lambda}_{ik} p_{ik}^*\right)} + \sum_{j=1}^{M} \nu_j^* \left\| \bar{\boldsymbol{w}}_{j,ik} \right\|_2^2 - \mu_{ik}^* = 0, \qquad \begin{matrix} i = 1, \dots, N \\ k = 1, \dots, \ell \end{matrix} \tag{3.56}$$

It can be seen that $\mu_{ik}$ is a slack variable that takes into account the non-negativeness of the powers $p_{ik}$, and it can be ommited to get the equation

$$\frac{-\hat{\lambda}_{ik}}{\log(2)\left(\sigma_i^2 + \hat{\lambda}_{ik} p_{ik}^*\right)} + \sum_{j=1}^{M} \nu_j^* \left\| \bar{\boldsymbol{w}}_{j,ik} \right\|_2^2 \geq 0, \qquad \begin{matrix} i = 1, \dots, N \\ k = 1, \dots, \ell \end{matrix} \tag{3.57}$$

Calling

$$L_{ik} = \sum_{j=1}^{M} \nu_j^* \left\| \bar{\boldsymbol{w}}_{j,ik} \right\|_2^2 \tag{3.58}$$

(3.57) can be solved for $p_{ik}^*$

$$p_{ik}^* \leq \frac{1}{\log(2)\, L_{ik}} - \frac{\sigma_i^2}{\hat{\lambda}_{ik}}, \qquad \begin{matrix} i = 1, \dots, N \\ k = 1, \dots, \ell \end{matrix} \tag{3.59}$$

The result in (3.59) resembles the classical *water-filling* solution, except that now the water level is not fixed, and it depends on the precoders. The coupling existing among the power constraints of the different BSs makes it impossible to find a closed-form solution for the values of $p_{ik}$.

Nevertheless, this analysis motivates the development of suboptimal schemes that are described in the following sections.

### 3.4.2 Modified Water-Filling

[27] proposes a simplification to the original problem, in order to make it more tractable. The coupling of the power constraints in (3.50) makes it impossible to get a simple solution for the optimal power allocation problem. [27] approaches the problem by first considering an equivalent virtual BS so that the problem is cast with a single power constraint.

In order to do so, instead of having a power constraint for each of the BSs consider a single power constraint given by the most restrictive BS in the original problem. Define

$$\Omega_{ik}^{\mathrm{BS}} = \max_{j=1,\dots,M} \left\| \bar{\boldsymbol{w}}_{j,ik} \right\|_2^2 \tag{3.60}$$

as the weights of the single virtual BS corresponding to each of the users' streams. The optimization problem becomes then

$$\begin{aligned} \underset{p_{ik}}{\text{minimize}} \quad & -\sum_{i=1}^{N}\sum_{k=1}^{\ell} \log_2\left(1+\frac{\hat{\lambda}_{ik}p_{ik}}{\sigma_i^2}\right) \\ \text{subject to} \quad & \sum_{i=1}^{N}\sum_{k=1}^{\ell} p_{ik}\Omega_{ik}^{\mathrm{BS}} - P_{\mathrm{BS,max}} \leq 0 \\ & -p_{ik} \leq 0, \qquad\qquad i=1,\dots,N \\ & \qquad\qquad\qquad\quad k=1,\dots,\ell \end{aligned} \tag{3.61}$$

where $P_{\mathrm{BS,max}}$ represents the most restrictive power constraint among all of the BSs.

This problem meets the same conditions as the original problem so that a similar analysis can be used. First formulate the Lagrangian of the new problem as

$$\begin{aligned} \mathcal{L}\left(\boldsymbol{p},\nu,\boldsymbol{\mu}\right) = & -\sum_{i=1}^{N}\sum_{k=1}^{\ell} \log_2\left(1+\frac{\hat{\lambda}_{ik}p_{ik}}{\sigma_i^2}\right) + \\ & \nu\left(\sum_{i=1}^{N}\sum_{k=1}^{\ell} p_{ik}\Omega_{ik}^{\mathrm{BS}} - P_{\mathrm{BS,max}}\right) - \\ & \sum_{i=1}^{N}\sum_{k=1}^{\ell} \mu_{ik}p_{ik} \end{aligned} \tag{3.62}$$

And its gradient is given by

$$\boldsymbol{\nabla}_{\boldsymbol{p}}\mathcal{L}\left(\boldsymbol{p}^*,\nu^*,\boldsymbol{\mu}^*\right) = \frac{-\hat{\lambda}_{ik}}{\log\left(2\right)\left(\sigma_i^2+\hat{\lambda}_{ik}p_{ik}^*\right)} + \nu^*\Omega_{ik}^{\mathrm{BS}} - \mu_{ik}^* = 0, \qquad \begin{matrix} i=1,\dots,N \\ k=1,\dots,\ell \end{matrix} \tag{3.63}$$

Using the KKT condition that the gradient of the Lagrangian should vanish, and considering $\mu_{ik}^*$ a slack variable, and solving for $p_{ik}^*$, the following inequality is obtained

$$p_{ik}^* \leq \frac{1}{\log(2)\,\nu^* \Omega_{ik}^{\mathrm{BS}}} - \frac{\sigma_i^2}{\widehat{\lambda}_{ik}}, \qquad \begin{matrix} i = 1, \ldots, N \\ k = 1, \ldots, \ell \end{matrix} \tag{3.64}$$

which, together with the constraint of the powers being non-negative, can be written as

$$p_{ik}^* = \left[ \frac{1}{\log(2)\,\nu^* \Omega_{ik}^{\mathrm{BS}}} - \frac{\sigma_i^2}{\widehat{\lambda}_{ik}} \right]^+, \qquad \begin{matrix} i = 1, \ldots, N \\ k = 1, \ldots, \ell \end{matrix} \tag{3.65}$$

The solution of this simplified problem is given by the water-filling solution with a variable water level and, in this case, an uncoupled solution for each of the data streams for each user. This allows for the use of standard and efficient methods to find the power allocation [22].

Clearly, the definition of the new problem makes it more restrictive than the original, and its solution will be also a feasible solution for the original problem, albeit not the optimal. The results in [27] show how under some conditions, the solution achieved like this can be rather close to the optimum one.

#### Standard Water-Filling

One further simplification that is done in [27] is to consider that, in practice, the values of all the $\Omega_{ik}^{\mathrm{BS}}$ are very similar to each other, so that it is possible to consider them equal. This turns the problem into a standard water-filling problem, with constant water level, where the solution is given by

$$p_{ik}^* = \left[ K_{\mathrm{WF}} - \frac{\sigma_i^2}{\widehat{\lambda}_{ik}} \right]^+, \qquad \begin{matrix} i = 1, \ldots, N \\ k = 1, \ldots, \ell \end{matrix} \tag{3.66}$$

where $K_{\mathrm{WF}} = \frac{1}{\log(2)\nu^* \Omega_{\mathrm{WF}}}$, is constant, as $\Omega_{ik}^{\mathrm{BS}} = \Omega_{\mathrm{WF}}\ \forall i = 1, \ldots, N;\ \forall k = 1, \ldots, \ell$ is the same for all the data streams of all the users.

### 3.4.3 Scaled Water-Filling

In [96] the same power allocation problem as in (3.50) is dealt with by considering a TPC, so that the optimization problem becomes

$$\begin{aligned} \underset{p_{ik}}{\text{minimize}} \quad & -\sum_{i=1}^{N}\sum_{k=1}^{\ell}\log_2\left(1+\frac{\hat{\lambda}_{ik}p_{ik}}{\sigma_i^2}\right) \\ \text{subject to} \quad & \mathrm{Tr}\left(\boldsymbol{W}^{(\mathrm{tx})}\boldsymbol{R_s}\boldsymbol{W}^{(\mathrm{tx}),H}\right)-MP_{\max}\leq 0 \\ & -p_{ik}\leq 0, \qquad\qquad i=1,\dots,N \\ & \qquad\qquad\qquad\quad k=1,\dots,\ell \end{aligned} \tag{3.67}$$

where it has been assumed that $P_{j,\max}=P_{\max}\forall j$.

Under this TPC, the solution is readily derived by water-filling [22], but the resulting $\boldsymbol{R}_{\boldsymbol{s}}^{\mathrm{TPC}}$ may violate the individual power contraints of each BS.

In order to meet each PBPC, the matrix $\boldsymbol{R}_{\boldsymbol{s}}^{\mathrm{TPC}}$ must be scaled so that the final power allocation is given by

$$\boldsymbol{R}_{\boldsymbol{s}}^{\mathrm{SWF}}=\beta\boldsymbol{R}_{\boldsymbol{s}}^{\mathrm{TPC}} \tag{3.68}$$

where the scaling factor $\beta\in(0,1)$ is calculated as

$$\beta=\frac{P_{\max}}{\max\limits_{j=1,\dots,M}\mathrm{Tr}\left(\boldsymbol{W}_j^{(\mathrm{tx})}\boldsymbol{R}_{\boldsymbol{s}}^{\mathrm{TPC}}\boldsymbol{W}_j^{(\mathrm{tx}),H}\right)} \tag{3.69}$$

The results in [96] show, as well, that this simplified approach can deliver near-optimum performance.

### 3.4.4 Uniform Power allocation

The simplest, both conceptually and computationally, alternative that can be considered to solve the power allocation in (3.50) consists in considering a uniform power allocation.

This approach assigns the same power to all the data streams of all the users. Formally this means

$$p_{ik}=p_s, \qquad \begin{matrix} i=1,\dots,N \\ k=1,\dots,\ell \end{matrix} \tag{3.70}$$

where the power $p_s$ should be computed taking into account the PBPC for each BS.

Recall from (3.45) the power transmitted by the $j$-th BS, where now the matrix $\boldsymbol{R_s}$ is given by

$$\boldsymbol{R_s} = p_s \boldsymbol{I} \tag{3.71}$$

and (3.45) becomes

$$p_s \operatorname{Tr}\left(\overline{\boldsymbol{W}}_j^{(\mathrm{tx})} \overline{\boldsymbol{W}}_j^{(\mathrm{tx}),H}\right) \leq P_{j,\max}, \quad j = 1, \dots, M \tag{3.72}$$

The new power allocation problem can be formulated as

$$\begin{aligned} &\underset{p}{\text{maximize}} && p \\ &\text{subject to} && p \operatorname{Tr}\left(\overline{\boldsymbol{W}}_j^{(\mathrm{tx})} \overline{\boldsymbol{W}}_j^{(\mathrm{tx}),H}\right) \leq P_{j,\max}, \qquad j = 1, \dots, M \end{aligned} \tag{3.73}$$

which is a *linear programming* optimization problem, and it can be solved efficiently using classical methods, e.g., bisection method [15].

# Chapter 4

# Mean Achievable Rates in Clustered Coordinated Base Station Transmission with Block Diagonalization*

## 4.1 Introduction

In Chapter 2 it has been discussed how global coordination in a cellular network is not feasible for practical application. Research has shown that grouping cells in clusters may help to alleviate some of the problems of global coordination. The clustering solution is not unique, though, and multiple alternatives and numerous parameters have to be chosen in order to meet different objectives.

The objective of this chapter is to analyze the mean achievable rate in a cellular network where clusters have been formed, and where BD is used within each cluster to manage the interference.

With this analysis, further research can be made in order to be able to choose from one of the most important parameters in clustering, the cluster size.

Numerical simulations are also performed in order to validate the theoretical analysis developed.

*The work shown in this chapter has been published in [24].

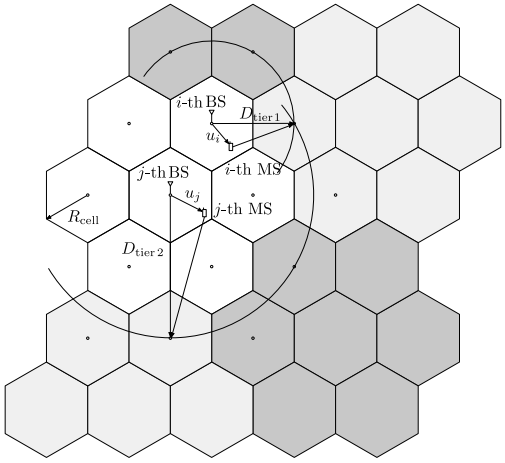


Figure 4.1: System layout with clusters of seven cells of radius $R_{\text{cell}}$ (the radius of the circle circumscribing the cell) with an example of two users, with the distances $D_{\text{tier 1}}$ and $D_{\text{tier 2}}$, respectively, from their BS to the interfering BSs.

## 4.2 Clustered Network

The network to be considered is organized as independent groups of $M$ cells, each of which is a cluster where its cells coordinate in order to transmit to the $N$ users that are located within the cluster.

The clusters that form the network are non-overlapping, i.e., each cell in the system belongs to one and only one cluster. Overlapping, user-centric clusters have been shown to provide, in some situations, better performance than disjoint clusters [9], but this approach gives rise to a dramatic increase of the management complexity.

The clusters, then, are defined by the network planner, and they are kept fixed, grouping the BSs according to a distance criterion, so that the cells belonging to a cluster must form, borrowing the name from graph theory, a *connected component* of the graph containing all the cells in the system.

In the setup under study, all the BSs in the cluster are considered cluster members, that is, no scheduling or adaptive selection of active BSs is addressed in this work. In any case, they could be considered as a special case of the optimization problem to obtain the power allocation scheme.

Figure 4.1 shows such a clustered network, where the disjoint clusters can be observed, together with other parameters that will be used in considering the interference for the analysis.

## 4.3 Interference Model

In Figure 4.1 an example of a network is shown, with three complete clusters of $M = 7$ cells each, and with some cells belonging to clusters not completely shown.

The user $i$, at a distance $d_i$ from its serving BS, *cf.* Section 3.1, is affected by the interference originated in the neighboring clusters. In this case, the closest interfering cells are located at a distance $D_{\text{tier 1}} = \sqrt{3}R_{\text{cell}}$ from the $i$-th BS.

Similarly, for the user $j$, at a distance $d_j$ from its serving BS, *cf.* Section 3.1, the nearest interfering cells are located at a distance $D_{\text{tier 2}} = 3R_{\text{cell}}$ from the $j$-th BS.

Due to the cellular geometry, for a cluster size of up to 18, only these two possibilities exist: the closest interfering cell is at a distance of either $D_{\text{tier 1}}$ or $D_{\text{tier 2}}$ from the serving BS of each user.

The hexagonal cell can be approximated by a circular one with radius $R_{\text{cell}}$, see Figure 4.1, and then, assuming a uniform distribution of the users over each cell, the probability density function (pdf) of the distance of a user to its serving (closest) BS is given by

$$f_{d_i}(d_i) = \frac{2d_i}{R_{\text{cell}}^2} \tag{4.1}$$

The interference power received at the user $i$ is equal to

$$I_i(d_i) = \sum_{m=1}^{M_{\text{interf}}} P_{\max} \hat{d}_{im}^{-\gamma} \tag{4.2}$$

where $M_{\text{interf}}$ is the number of interfering BSs, i.e., the total number of cells in the system minus the $M$ cells that form the cluster, and $\hat{d}_{im}$ is the distance from the $m$-th BS outside the cluster to the $i$-th user in the cluster. All the interfering BSs are assumed to be transmitting at full power.

In order to simplify the computation of the interference power, an equivalent model is introduced. In this model, the interference comes from $M_{\text{eq},i}$ cells, all of which are located at the same distance $(D_i - d_i)$ from the $i$-th user, the one being interfered.

The distance $D_i$ takes the value of the distance from the serving BS to the closest interfering BS

$$D_i \in \{D_{\text{tier 1}}, D_{\text{tier 2}}\} \tag{4.3}$$

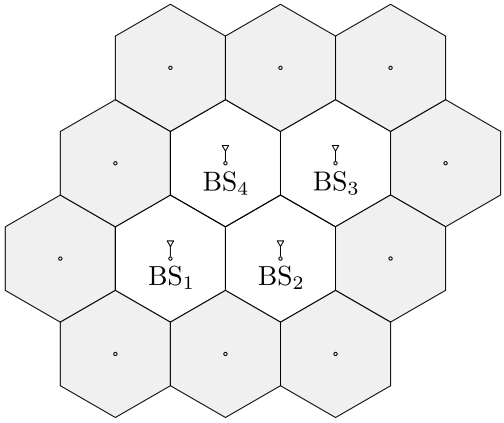


Figure 4.2: Cluster with $M = 4$ cells and neighbor interfering cells.

The equivalent number of interfering BSs, $M_{\mathrm{eq},i}$, is such that the total interference power is the same as in the original layout.

With all this, (4.2) can be written as

$$I_i\left(d_i\right) = P_{\max} M_{\mathrm{eq},i}\left(D_i - d_i\right)^{-\gamma} \tag{4.4}$$

This approach is similar to that followed in [19], where a fluid model network is used. This model assumes that there is a continuum of BSs interfering, but this will not be considered in the current work for the sake of simplicity.

The real and equivalent model produce the same total interference, provided that $M_{\mathrm{eq},i}$ is adequately selected.

In order to determine $M_{\mathrm{eq},i}$ the only interference that is accounted for is the one coming from the first tier of neighboring cells. This implies that different cluster configurations may have different number of interfering BSs for each of the cells in the cluster, and this number for the $i$-th cell is denoted as $M_{\mathrm{int},i} \leq M_{\mathrm{interf}}$.

This is made clear in Figure 4.2 where a cluster with $M = 4$ cells is surrounded by $M_{\mathrm{interf}} = 12$ cells. In this cluster, cells 1 and 3 experience an interference coming from $M_{\mathrm{int},1} = M_{\mathrm{int},3} = 4$ neighboring cells, while cells 2 and 4 receive the interference from $M_{\mathrm{int},2} = M_{\mathrm{int},4} = 3$ cells.

In order to approximate the value of equivalent interfering BSs for a general network setup, first a simple scenario Figure 4.3 is considered, with a cluster of $M = 1$ cells, where a single user, $i = 1$, in the cell is affected by an interference power $I_1$ coming from all the $M_{\mathrm{int},1} = 6$ belonging to the first tier.

An assumption that can be made is that half of the $M_{\mathrm{int},1}$, i.e., three, BSs are

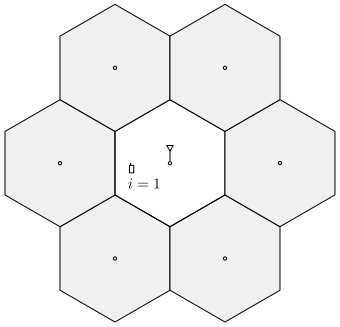


Figure 4.3: Simple scenario with a single cluster of $M = 1$ cell, and the six interfering cells surrounding it.

located at a distance $(D_1 - d_1)$ and the other half are located at a distance $(D_1 + d_1)$. Accordingly, the interference power can be expressed as

$$I_1(d_1) = P_{\max}\left[\frac{3}{(D_1 + d_1)^{\gamma}} + \frac{3}{(D_1 + d_1)^{\gamma}}\right] \tag{4.5}$$

which is equal to (4.4) if the equivalent number of interfering BSs is defined as

$$M_{\mathrm{eq},1} = 3\left[1 + \left(\frac{D_1 - d_1}{D_1 + d_1}\right)^{\gamma}\right] \tag{4.6}$$

In general, if a user $i$ is considered to have $M_{\mathrm{int},i}$ interfering BSs in the first tier at a distance $D_i$, defined as in (4.3), then the equivalent number of interfering BSs is given by

$$M_{\mathrm{eq},i} \approx \frac{M_{\mathrm{int},i}}{2}\left[1 + \left(\frac{D_i - d_i}{D_i + d_i}\right)^{\gamma}\right] \tag{4.7}$$

In order to evaluate (4.7), it is possible to set the distance $d_i$ to the average distance of the user within the cell. A similar approach is used in [73] to characterize the statistics of the interference in a multicell scenario. This average distance can be obtained from the uniform spatial distribution in (4.1) as

$$\mathbb{E}\{d_i\} = \frac{2}{3}R_{\mathrm{cell}} \tag{4.8}$$

and then

$$M_{\mathrm{eq},i} \approx \frac{M_{\mathrm{int},i}}{2}\left[1+\left(\frac{D_i-\frac{2}{3}R_{\mathrm{cell}}}{D_i+\frac{2}{3}R_{\mathrm{cell}}}\right)^{\gamma}\right] \tag{4.9}$$

Section 4.5 deals with the comparison between simulations and the analytical results, showing that the approximation in (4.9) is accurate.

## 4.4 Analysis of the Rate

In the case of having global coordination or, equivalently, having only one cluster including all the BSs, the interference among the users is completely eliminated through the use of BD, *cf.* Section 3.3. On the other hand, in a multicluster environment, it is necessary to consider the effect of the interference coming from the cells outside the cluster. Hence, the mean achievable rate in (3.39) becomes (dropping the expectation notation)

$$R_i^{\mathrm{BD}} = \sum_{k=1}^{\ell} \log_2\left(1+\frac{\widehat{\lambda}_{ik}p_{ik}}{\sigma_i^2+I_i}\right) \tag{4.10}$$

where the parameter $I_i$ represents the average power of the total interference contributions received in each data stream of user $i$ from the interfering BSs.

It can be seen in (4.10) that the rate depends on the distance $d_i$ of each user's equipment from the center of its cell. Using the pdf in (4.1) the average of the rate over all possible locations, making explicit the dependence on the distance $d_i$, can be expressed as

$$\begin{aligned}\bar{R}_i^{\mathrm{BD}} &= \int_0^{R_{\mathrm{cell}}} R_i^{\mathrm{BD}}(u)\,\frac{2u}{R_{\mathrm{cell}}^2}\mathrm{d}u \\ &= \int_0^{R_{\mathrm{cell}}} \sum_{k=1}^{\ell} \log_2\left(1+\frac{\widehat{\lambda}_{ik}(u)\,p_{ik}}{\sigma_i^2+I_i(u)}\right)\frac{2u}{R_{\mathrm{cell}}^2}\mathrm{d}u\end{aligned} \tag{4.11}$$

In (4.11) there are three parameters that determine the overall average rate, namely

- The interference $I_i(d_i)$ coming from outside the cluster.
- The effect of the channel fading and of the path loss, represented by the term $\widehat{\lambda}_{ik}(d_i)$.
- The power $p_{ik}$ assigned to the $k$-th data stream of user $i$.

In the following, the characterization of each of these parameters will be approached separatedly.

### 4.4.1 Interference

As described in Section 4.3 the contribution of interference, $I_i\,(d_i)$ on each data stream of user $i$, coming from the cells outside the cluster, can be considered as generated by an equivalent number of BSs located all of them at a distance of $D_i - d_i$ from the user. Recall that, for clusters of size up to 18, $D_i$ can take one of two values as in (4.3).

The interfering distance $D_i$ is then normalized to the cell radius $R_{\text{cell}}$ by setting

$$\bar{d}_i = \frac{D_i}{R_{\text{cell}}} \tag{4.12}$$

In expression (4.10) it is assumed that the interference can be treated as Gaussian noise, so that the power is calculated as the variance of that noise. Throughout the simulations that were performed, it has been found that, on average, at least 25 out-of-cluster cells contributed with significant interference.[†]

This number of 25 is dependent on the simulation paremeters, but it gives an idea of the order of magnitud of interferers present, and it justifies the treatment of the interference as Gaussian noise, by virtue of the central limit theorem [72].

### 4.4.2 Fading Effect

The terms $\hat{\lambda}_{ij}$ are the squared diagonal values of the matrix $\widehat{\boldsymbol{\Lambda}}_i$, *cf.* Section 3.3. This matrix is obtained in (3.36) by the combination of the channel matrix $\boldsymbol{H}_i$ and a unitary matrix, $\widetilde{\boldsymbol{V}}_i^{(0)}$.

The channel matrix $\boldsymbol{H}_i$ is composed of the submatrices $\boldsymbol{H}_{ij}$, where the fading elements have a power path loss of $d_{ij}^{-\gamma}$, and the elements of $\boldsymbol{H}_{ij}$ are independent from the elements of $\boldsymbol{H}_{ik}$ for all $j$ different from $k$.

It is possible to define an alternative set of coefficients $\kappa_{ij}$ that do not include the path loss effect

$$\kappa_{ij} \triangleq \frac{\hat{\lambda}_{ij}}{d_i^{-\gamma}} \tag{4.13}$$

[†]Being significant defined as being greater than the power received at the cell edge.

These coefficientes are the elements of the main diagonal of the matrix

$$d_i^{\gamma} \widehat{\boldsymbol{\Lambda}}_i \widehat{\boldsymbol{\Lambda}}_i^H \tag{4.14}$$

And it can be seen that these diagonal elements are the singular values of the matrix

$$d_i^{\gamma} \boldsymbol{H}_i \widetilde{\boldsymbol{V}}_i^{(0)} \widetilde{\boldsymbol{V}}_i^{(0),H} \boldsymbol{H}_i^H \tag{4.15}$$

where $\boldsymbol{H}_i$ has Gaussian entries, and $\widetilde{\boldsymbol{V}}_i^{(0)}$ is a unitary matrix.

In the case of having $Mt = Nr$, the coefficientes $\kappa_{ij}$ are the eigenvalues of a Wishart matrix while, in the general case of $Mt \geq Nr$ the matrix in (4.15) can be approximated by a Wishart matrix. Through simulations, it has been verified that the mean of the eigenvalues of both matrices, the original in (4.15) and the approximate Wishart, is the same and the difference between the two Cumulative Distribution Function (CDF) is less than 10 %.

The joint pdf of the eigenvalues $\kappa_{ij}$ of a Wishart matrix can be obtained when the columns of the corresponding Gaussian matrix have an identity covariance matrix

$$\boldsymbol{\Sigma}_i = \boldsymbol{I} \tag{4.16}$$

and it is given by [87]

$$f_{\kappa_{i1},\dots,\kappa_{i\ell}}(\kappa_{i1},\dots,\kappa_{i\ell}) = e^{-\sum_{k=1}^{\ell}\kappa_{ik}} \prod_{k=1}^{\ell} \frac{1}{[(\ell-k)!]^2} \prod_{m=k+1}^{\ell} (\kappa_{im}-\kappa_{i\ell})^2 \tag{4.17}$$

However, in the evaluation of the rate the complete pdf is not needed, and only the sum

$$\sum_{i=1}^{N}\sum_{k=1}^{\ell} \log(\kappa_{ik}) \tag{4.18}$$

is required, which represents the expectation of the logarithm of the determinant, for which results are available, also for the general case when the covariance matrix is different from the identity, $\boldsymbol{\Sigma} \neq \boldsymbol{I}$, and it is given by [87]

$$\mathbb{E}\left\{\sum_{i=1}^{N}\sum_{k=1}^{\ell} \log(\kappa_{ik})\right\} = \sum_{m=1}^{N\ell} \psi(N\ell - m) + \log(|\boldsymbol{\Sigma}|) \tag{4.19}$$

where $\psi(\cdot)$ is the Euler's digamma function [36], and where the matrix $\boldsymbol{\Sigma}$ is

$$\boldsymbol{\Sigma} = \begin{bmatrix} \boldsymbol{\Sigma}_1 & \mathbf{0} & \cdots & \mathbf{0} \\ \mathbf{0} & \boldsymbol{\Sigma}_2 & \cdots & \mathbf{0} \\ \vdots & \vdots & \ddots & \vdots \\ \mathbf{0} & \mathbf{0} & \cdots & \boldsymbol{\Sigma}_N \end{bmatrix} \tag{4.20}$$

with $\boldsymbol{\Sigma}_i$ the covariance matrix of the columns of the matrix $d_i^{\gamma/2}\boldsymbol{H}_i\widetilde{\boldsymbol{V}}_i^{(0)}$

$$\boldsymbol{\Sigma}_i = \boldsymbol{I}\left[1 + \sum_{\substack{j=1 \\ j\neq i}}^{M} \left(\frac{d_i}{d_{ij}}\right)^{\gamma}\right] \tag{4.21}$$

It is possible to define a parameter $G_i$

$$G_i \triangleq 1 + \sum_{\substack{j=1 \\ j\neq i}}^{M} \left(\frac{d_i}{d_{ij}}\right)^{\gamma} \tag{4.22}$$

that can be considered as a cluster gain. Its value can be approximated considering the average distance of a user to its BS (4.8), and the distance from the rest of the BSs in the cluster to be either $D_{\text{tier 1}}$ or $D_{\text{tier 2}}$. If additionally these two distances are normalized by the average distance in (4.8)

$$\begin{aligned} \overline{D}_{\text{tier 1}} &\triangleq \frac{3D_{\text{tier 1}}}{2R_{\text{cell}}} \\ \overline{D}_{\text{tier 2}} &\triangleq \frac{3D_{\text{tier 2}}}{2R_{\text{cell}}} \end{aligned} \tag{4.23}$$

then the gain factor $G_i$ can be approximated for different cluster sizes as

$$G_i = \begin{cases} 1 + \frac{M-1}{2}\left[\left(\frac{1}{\overline{D}_{\text{tier 1}}-1}\right)^{\gamma}\left(\frac{1}{\overline{D}_{\text{tier 1}}+1}\right)^{\gamma}\right] & M \leq 7 \\ 3\left[\left(\frac{1}{\overline{D}_{\text{tier 1}}-1}\right)^{\gamma}\left(\frac{1}{\overline{D}_{\text{tier 1}}+1}\right)^{\gamma}\right]\frac{M-7}{2}\left[\left(\frac{1}{\overline{D}_{\text{tier 2}}-1}\right)^{\gamma}\left(\frac{1}{\overline{D}_{\text{tier 2}}+1}\right)^{\gamma}\right] & 7 < M \leq 18 \end{cases} \tag{4.24}$$

In Figure 4.4 a fixed distance for the users equal to $d_i = 2/3 R_{\text{cell}}$, (4.8), is considered and the values of the sum of the natural logarithm of the values $\kappa_{ij}$ are calculated through simulations and using the expression (4.19), for the case of $t = r = 2$.

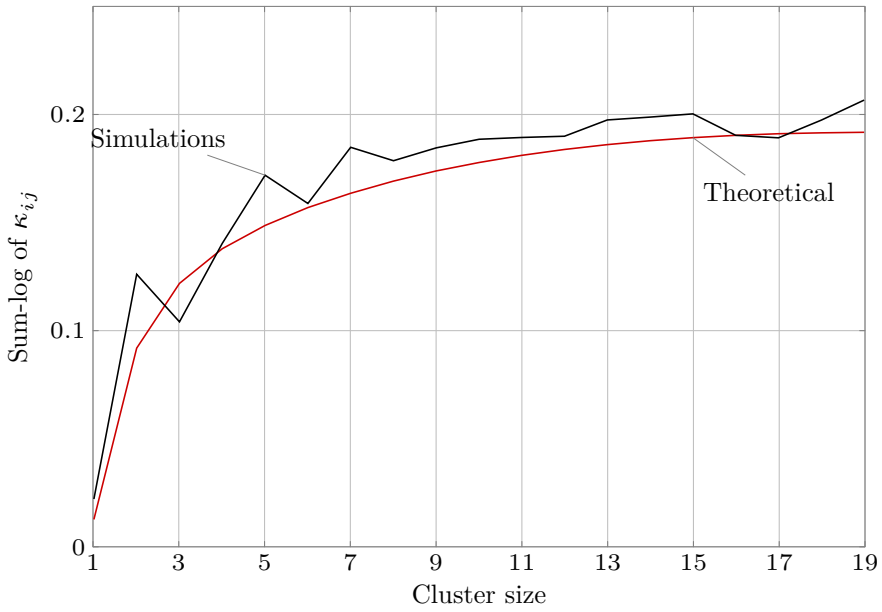


Figure 4.4: Sum-log of the terms $\kappa_{ij}$. Comparison between simulations and the values obtained using (4.19) for $t = r = 2$.

It can be seen how the sum of the log values of $\kappa_{ij}$ presents a diminishing increase as the cluster size $M$ increases. This can be explained by a reduced contribution of the BSs, that are farther than in smaller clusters, which becomes negligible due to the path loss.

Notice that, in the evaluation of the mean achievable rate, a factor $1/N$ is applied in order to evaluate the average rate per user, taking into consideration that in a cluster with more cells, there would be more users as well.

Thus, a decrease occurs in the mean achievable rate per user for large values of $M$, as it will be shown in Section 4.5.

### 4.4.3 Power allocation

Under the BD strategy, the transmission within each cluster is equivalent to a set of parallel non-interfering channels.

Therefore, the transmission power must be allocated in order to optimize some quality of service parameters, such as the sum-rate or a weighted sum of the rates, for the users of each cluster.

This objective is subject to a maximum transmission power available at each BS, (3.45) and (3.48)

$$\sum_{i=1}^{N}\sum_{k=1}^{\ell} p_{ik}\left\|\bar{\boldsymbol{w}}_{j,ik}\right\|_2^2 \leq P_{\max} \tag{4.25}$$

for each of the $M$ BSs in the cluster.

The rate maximization problem is described in more detail in Section 3.4, and the solutions range from the simplest uniform power allocation, *cf.* Subsection 3.4.4, to an optimal allocation, *cf.* Subsection 3.4.1. In any case, the problem of power allocation is not the focus of this work because it can be solved separately and the actual powers could be inserted in the analytical expressions developed.

Hence, in the following a theoretical framework is derived for the uniform power allocation scheme, for the sake of simplicity, and an example with a different power allocation will be presented with the results.

With a uniform power allocation a common average power $p_s$ is used for every stream of every user, as seen in (3.70). This value $p_s$ varies according to the number of BSs in the cluster, decreasing for a larger size of the cluster, since a fraction of the overall available power is spent in the coordination, to null the interference.

Substituting all the $p_{ik}$ in (4.25) for the common value $p_s$ it is easy to see that the condition in (4.25) is limited by the BS for which the following factor is maximum

$$\chi_j \triangleq \sum_{i=1}^{N}\sum_{k=1}^{\ell}\left\|\bar{\boldsymbol{w}}_{j,ik}\right\|_2^2 \tag{4.26}$$

Assuming that the coefficients of the precoding matrix, i.e., the elements of the vector $\bar{\boldsymbol{w}}_{j,ik}$, are Gaussian, then $\chi_j$ is a Chi-squared random variables with $N' \triangleq N\ell t$ degrees of freedom, and the power $p_s$ is related to the reciprocal value of the maximum of $M$ random variables

$$p_s = \frac{P_{\max}}{\mathbb{E}\{\chi\}} \tag{4.27}$$

with

$$\chi = \max\{\chi_1, \ldots, \chi_M\} \tag{4.28}$$

Then the probability distribution function of $\chi$ is given by

$$F_{\chi}(x) = P(N', x)^M \tag{4.29}$$

where $P(\cdot,\cdot)$ is the regularized Gamma function.

The mean value can be derived from the probability distribution function in (4.29) as

$$\mathbb{E}\{\chi\} = \int_0^\infty \left(1 - F_\chi(x)\right) \mathrm{d}x \tag{4.30}$$

and it can be bounded using

$$(1 - e^{-\alpha x})^a \leq P(a, x) \leq \left(1 - e^{-\beta x}\right)^a \tag{4.31}$$

with

$$\begin{aligned} \alpha &= \begin{cases} 1 & 0 < a < 1 \\ \Gamma(a+1)^{-\frac{1}{a}} & a > 1 \end{cases} \\ \beta &= \begin{cases} \Gamma(a+1)^{-\frac{1}{a}} & 0 < a < 1 \\ 1 & a > 1 \end{cases} \end{aligned} \tag{4.32}$$

where $\Gamma(\cdot)$ is the Gamma function.

The average value of $\chi$ is then bounded by

$$\frac{1}{\beta}\left[\psi(Mt+1) + \gamma_0\right] \leq \mathbb{E}\{\chi\} \leq \frac{1}{\alpha}\left[\psi(Mt+1) + \gamma_0\right] \tag{4.33}$$

with $\psi(\cdot)$ again the Euler's digamma function, and $\gamma_0$ the Euler-Mascheroni constant.

It is possible to rewrite (4.33) in terms of $p_s$ as

$$P_{\max} \frac{\Gamma(N'+1)^{-\frac{1}{N'}}}{\psi(Mt+1) + \gamma_0} \leq p_s \leq P_{\max} \frac{1}{\psi(Mt+1) + \gamma_0} \tag{4.34}$$

In the evaluation of the rate, the lower bound in (4.34) will be considered, providing a lower bound to the average rate of each user.

The bounds for the power per stream $p_s$ in (4.34) are compared in Figure 4.5 with the results obtained through simulations.

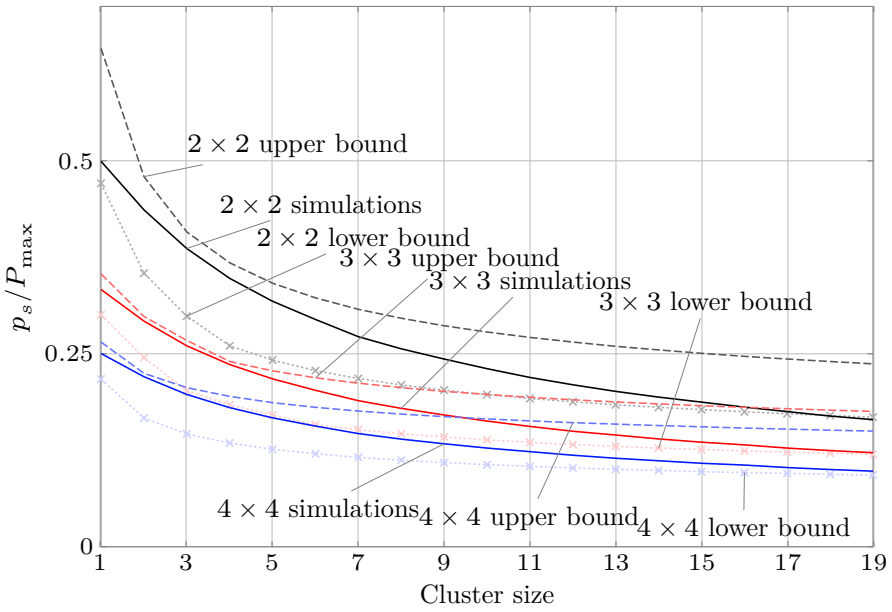


Figure 4.5: Normalized average power per stream $p_s/P_{\max}$ for different antenna configurations: comparison between simulations and the bounds in (4.34).

First thing that can be seen in Figure 4.5 is how the power $p_s$ decreases with the size of the cluster, and this affects the mean achievable rate as it will be discussed in Section 4.5.

Secondly, Figure 4.5 shows a very good agreement between the analytical and simulation results for different antenna configurations. In particular, the upper bound is tight for small clusters while the lower bound becomes more accurate for bigger clusters.

### 4.4.4 Evaluation of the mean achievable rate

The performance of the coordination scheme will be measured by the mean achievable rate per user in the cluster

$$\bar{R}^{\mathrm{BD}} = \frac{1}{N}\sum_{i=1}^{N} \bar{R}_i^{\mathrm{BD}} \tag{4.35}$$

It is possible to derive a lower bound for each user's average rate in (4.11) by considering the inequality

$$\log(1+x) \geq \log(x) \tag{4.36}$$

so that the average rate for the $i$-th user (4.11) becomes

$$\begin{aligned}\bar{R}_i^{\mathrm{BD}} &\geq \frac{1}{\log(2)} \sum_{k=1}^{\ell} \int_0^{R_{\mathrm{cell}}} \log\left(\frac{p_{ik}\kappa_{ik}u^{-\gamma}}{\sigma_i^2 + P_{\max} M_{\mathrm{eq},i}\left(D_i - u\right)^{-\gamma}}\right) \frac{2u}{R_{\mathrm{cell}}^2}\mathrm{d}u \\ &= \frac{1}{\log(2)} \sum_{k=1}^{\ell} \left\{ \log\left(\kappa_{ik}\right) + \log\left(\frac{p_{ik}}{P_{\max}}\right) + Z_i \right)\end{aligned} \tag{4.37}$$

where the interference model has been introduced, and $Z_i$ is defined as

$$Z_i \triangleq \int_0^{R_{\mathrm{cell}}} \log\left(\frac{u^{-\gamma}}{\frac{\sigma_i^2}{P_{\max}} + M_{\mathrm{eq},i}\left(D_i - u\right)^{-\gamma}}\right) \frac{2u}{R_{\mathrm{cell}}^2}\mathrm{d}u \tag{4.38}$$

The value of $Z_i$is derived in Appendix A, and it is

$$\begin{aligned} Z_i = {} & \frac{\gamma}{2} + \log(\rho) + \bar{d}_i^2 \log\left(\frac{\bar{d}_i^{\gamma}}{M_{\mathrm{eq},i}\rho + \bar{d}_i^{\gamma}}\right) \\ & - 2\bar{d}_i^2 \gamma\, {}_2\mathrm{F}_1\left(1, \frac{1}{\gamma}; \frac{\gamma+1}{\gamma}; \frac{-\bar{d}_i^{\gamma}}{M_{\mathrm{eq},i}\rho + \bar{d}_i^{\gamma}}\right) \\ & + \frac{\bar{d}_i^2}{2} \gamma\, {}_2\mathrm{F}_1\left(1, \frac{2}{\gamma}; \frac{\gamma+2}{\gamma}; \frac{-\bar{d}_i^{\gamma}}{M_{\mathrm{eq},i}\rho + \bar{d}_i^{\gamma}}\right) \\ & - \left(\bar{d}_i^2 - 1\right) \log\left(\frac{\left(\bar{d}_i - 1\right)^{\gamma}}{M_{\mathrm{eq},i}\rho + \left(\bar{d}_i - 1\right)^{\gamma}}\right) \\ & + 2\bar{d}_i \left(\bar{d}_i - 1\right) \gamma\, {}_2\mathrm{F}_1\left(1, \frac{1}{\gamma}; \frac{\gamma+1}{\gamma}; \frac{-\left(\bar{d}_i - 1\right)^{\gamma}}{M_{\mathrm{eq},i}\rho}\right) \\ & - \frac{\left(\bar{d}_i - 1\right)^2}{2} \gamma\, {}_2\mathrm{F}_1\left(1, \frac{2}{\gamma}; \frac{\gamma+2}{\gamma}; \frac{-\left(\bar{d}_i - 1\right)^{\gamma}}{M_{\mathrm{eq},i}\rho}\right) \end{aligned} \tag{4.39}$$

where ${}_2\mathrm{F}_1\left(\cdot\right)$ is the hypergeometric function, and $\rho$ is the SNR as defined in (3.25).

Combining (4.19), (4.34), (4.35), and (4.37) the analytical expression for the mean achievable rate per user is

$$\bar{R}^{\mathrm{BD}} \geq \frac{1}{N\log(2)}\left[\log\left(|\boldsymbol{\Sigma}|\right) + \sum_{m=1}^{N\ell}\psi\left(N\ell - m\right) + N\ell\log\left(\frac{\Gamma\left(N'+1\right)^{-\frac{1}{N'}}}{\psi\left(Mt+1\right)+\gamma_0}\right) + \ell\sum_{i=1}^{N} Z_i\right] \tag{4.40}$$

## 4.5 Numerical Results

In this section, the results derived from the analytical expression in (4.40) are compared with the results obtained through simulations.

The scenario for the simulations is a network composed of 169 cells, laid out as 7 concentric tiers of hexagonal cells.

The cell radius, unless stated otherwise, is assumed to be $R_{\mathrm{cell}} = 1.4\,\mathrm{km}$.

All the results are averaged over 5,000 random trials. In each of these trials the position of the users was randomly set according to a uniform distribution inside each cell, Section 4.3. Also, for each of the trials, a random channel was generated according to the model described in Section 3.2, with a path loss exponent of $\gamma = 3.8$.

The parameter evaluated in the simulations is the achievable rate defined in (4.10), in which the different variables required (transmission power, interference power, $\hat{\lambda}_{ik}$, etc) were obtained by simulations.

As it has already been mentioned, the clusters considered are static, i.e., they are fixed and do not change for all the simulations. Despite this, not all the clusters must have the same shape for the same cluster size $M$. In fact, in the simulations, the clusters were generated following a heuristic approach that tries to group cells in a compact way, with a regular shape, by minimizing the sum of the inter-cell distances, thus to avoid long clusters. Note, however, that some values of $M$ do not allow for regular clusters, i.e., hexagonal, to be formed. Figure 4.6 shows an example of this situation, where not all the clusters have the same shape.

### 4.5.1 Analytical and simulation results comparison

In order to validate the analytical expression (4.40), first it is compared with the mean achievable rate simulated using BD. The Minimum Mean Squared Error (MMSE) precoder described in [78] is also included in the comparison, for the sake of completeness, although the analytical derivations did not consider it.

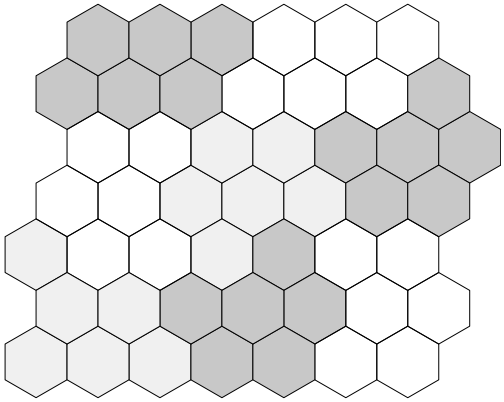

Figure 4.6: Irregular shaping of the clusters, due to the heuristic clustering algorithm used.

The antenna configuration used for this first comparison is $r = t = 2$, and also different values of the SNR, as defined in (3.25), are used so to observe the behaviour in different SNR regimes.

Figure 4.7 shows the mean achievable rate as a function of the cluster size $M$.

As expected, the MMSE approach outperforms the BD strategy at low SNR. On the other hand, for moderate values of the SNR BD is able to provide comparable, and even more favorable, results, thus showing that the interference dominates over the noise for regimes other than the low SNR regime.

A very good agreement between the theoretical result in (4.40) and the simulations is clear in Figure 4.7, where also some variations can be seen in the simulation results. This is mainly due to the variability of the cluster shape, as seen in Figure 4.6, for different cluster sizes, and not to a low number of simulations that were averaged. That irregular shape of the clusters, despite being more or less controlled in the heuristic cluster selection algorithm, affects the simulation results in the form of the variability shown in the figures.

[62] points out at a fundamental limit of cooperation, and it is shown how the gains from cooperation cannot be unbounded, and that increasing the number of coordinated elements may saturate the performance achieved. This very same behaviour can be observed in Figure 4.7, both for BD and MMSE, where the mean achievable rate do not grow unboundedly with the cluster size, and an optimum value of the size $M$ can be found.

Figure 4.8 also shows a similar behaviour. In this case, the mean achievable rate is represented as a function of the SNR, and there is an SNR at which the rate stops growing. This threshold SNR depends on the propagation path loss exponent $\gamma$ because it directly determines the influence of the interference. In particular, the saturation SNR for BD is higher than for MMSE. For the former, it is always above 20 dB, for

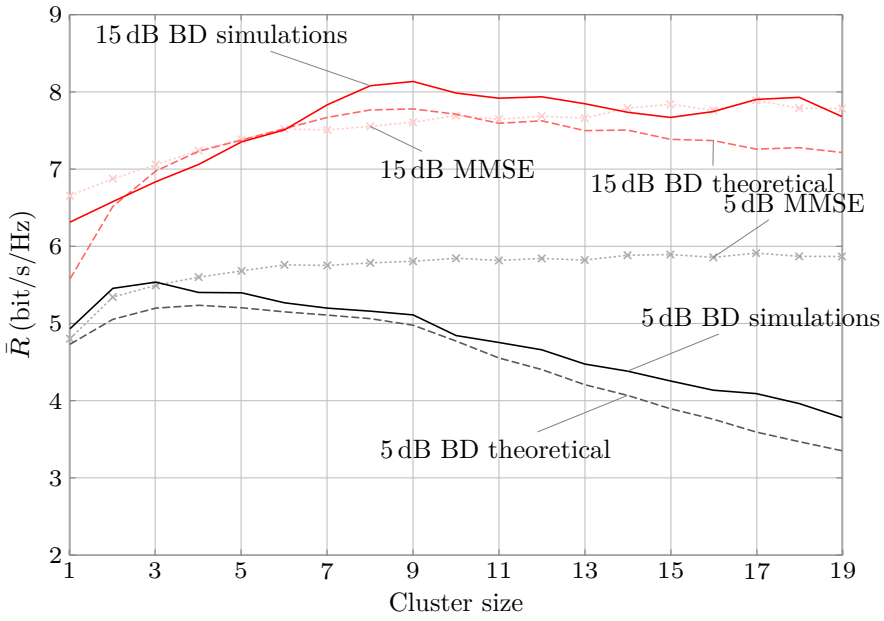


Figure 4.7: Mean achievable rate per user as a function of the number of cells in the cluster for $r = 2$, $t = 2$, variable values of SNR, $\gamma = 3.8$.

the scenarios considered, even for very small path loss exponents. This means that the saturation occurs for relatively large values of the SNR which is of practical importance because it would be possible to deliver good performance, using BD, within a practical range of SNR values.

Under the restriction that the same $P_{\max}$ is transmitted for all values of $\gamma$, the saturation occurs at different levels for each $\gamma$, although the general conclusions do not change.

In order to complete the validation of the theoretical results with the simulations, a fixed value of SNR= 25 dB and different antenna configurations were considered in Figure 4.9, still using uniform power allocation. The discrepancies between the theoretical results and the simulations are not only due to the approximations, but also to the fact that in the simulation scenario not all the clusters have the same shape, despite having the same number of cells.

### 4.5.2 Effect of the power allocation

The cause of the decrease of the rate with respect to the cluster size, as seen in Figure 4.7, is two-fold:

- First, the value of the attenuation experienced by each data stream, $\hat{\lambda}_{ik}$ decreases when the size of the cluster increases, as shown in Figure 4.4.

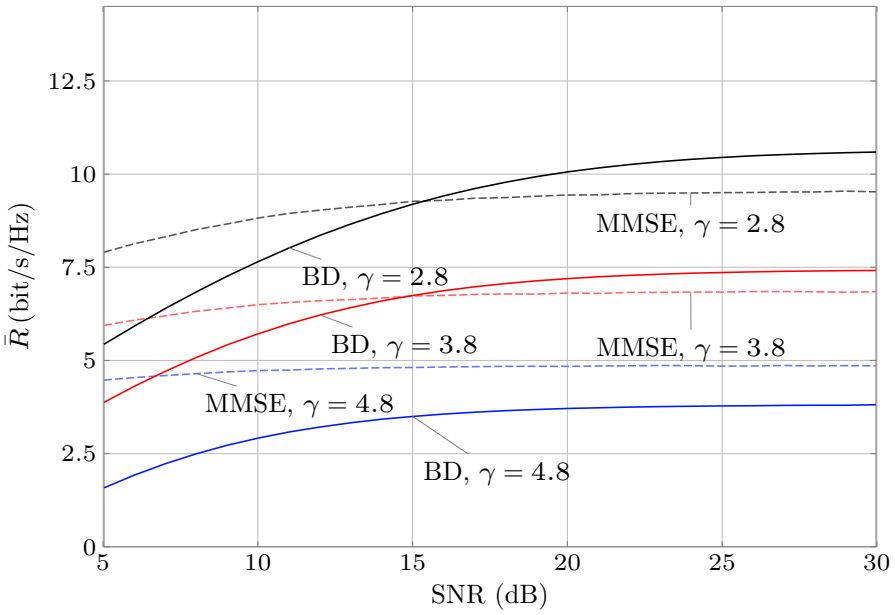


Figure 4.8: Mean achievable rate as a function of the SNR for different values of the path loss coefficient $\gamma$, for $r = 2$, $t = 2$ and $M = 7$.

- Second, the power assigned to each data stream, the terms $p_{ik}$ that for a uniform power allocation are all equal to $p_s$, also decreases as the cluster grows, Figure 4.5, due to a coordination "loss".

In this section, a different power allocation scheme, other than the uniform, was used in order to verify if the behavior observed in Figure 4.7, where the rate decreases with the cluster size, is due to the power allocation.

The optimal power allocation used was obtained by means of numerical optimization, as described in [27], using CVX [37], [38], and those powers were plugged into (4.40) instead of the uniform power allocation.

In Figure 4.10 the rates obtained with the uniform and the optimum power allocation are compared and represented versus the size of the cluster.

Although, as expected, the optimal outperforms the uniform power allocation, both curves show a similar trend, meaning that a reduced growth of the rate (and in some situationes a reduction of the rate itself) is not due to the power allocation scheme, but it is the manifestation of a fundamental limitation of the coordination scheme, along the lines of the results in [62].

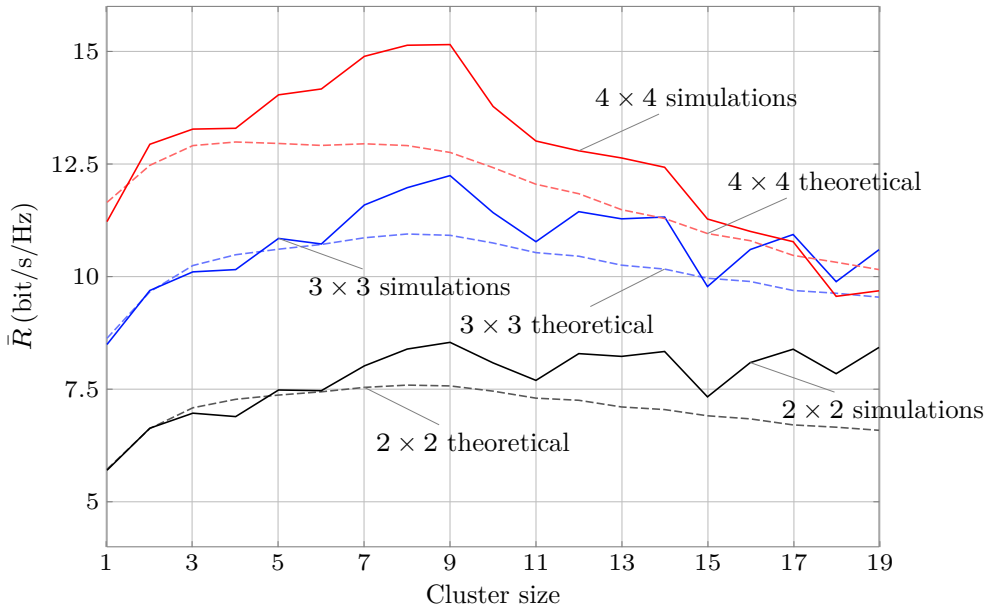


Figure 4.9: Mean achievable rate per user as a function of the cluster size for SNR= 25 dB, $\gamma = 3.8$ and different antenna configurations.

### 4.5.3 Optimum cluster size

Figure 4.7 through Figure 4.10 show a common trend which is the rate having a reduced growth, or even a reduction, with the cluster size.

Given this, it is possible and interesting to find the cluster size $M$ that can maximize the mean achievable rate.

In the case of the rate actually decreasing with $M$, the optimum value can be readily obtained as the value of $M$ for which the maximum rate is obtained.

In some of the simulations results, the rate does not decrease within the range of cluster sizes that were simulated, so it is not possible, with the simulation conditions used, to find a maximum for the mean achievable rate. Something that can be observed, nevertheless, is that its growth with $M$ is diminished so that the optimum value of $M$ can be calculated by considering the relative change of the rate. The optimum is assumed to be found when the marginal increase of the rate is bellow a given percentage. In the case under study, the threshold was set to a 10 %.

Figure 4.11 represents the optimum value of $M$ as a function of the SNR, for different antenna configurations, and for the power allocation schemes considered until now, uniform and optimum.

It can be seen that, for a wide range of SNR, the optimum value is limited to around 7–10 cells.

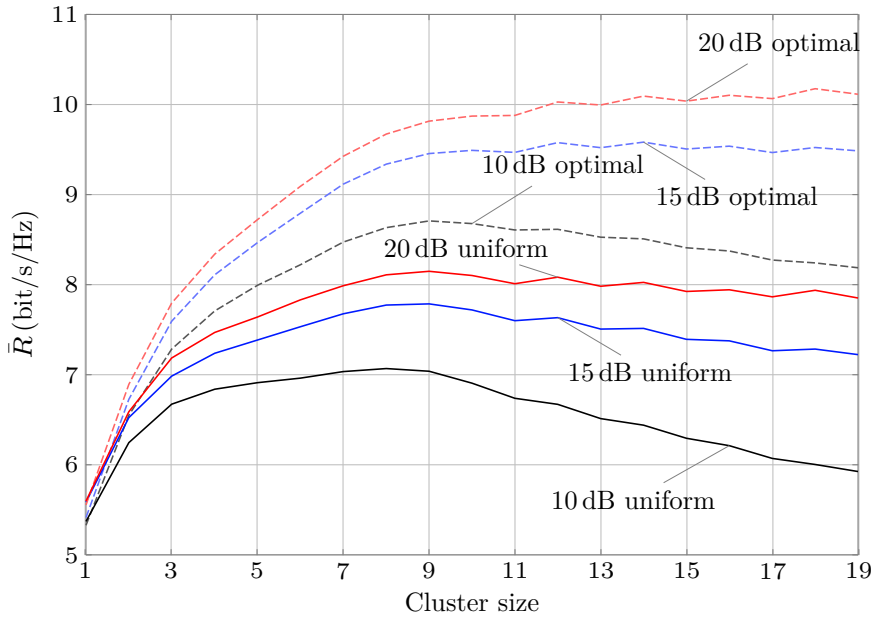


Figure 4.10: Comparison between different power allocation schemes, namely uniform and optimal. Mean achievable rate per user as a function of the cluster size for $r = t = 2$, $\gamma = 3.8$ and different values of SNR.

Only for high SNR is it more convenient to increase the cluster size, since the reduction of the interference can compensate the decrease of the cluster gain due to the decrease of the factors $\widehat{\lambda}_{ik}$. This only happens for the case of considering the optimal power allocation, because in the case of the uniform power scheme there is the additional decrease of the power allocated to each stream, $p_s$.

### 4.5.4 Effect of signaling overhead

It is common in the literature to not take into account the effect of the signaling overhead, and the same has been done in all the previous results of this work.

However, if a certain percentage of the available resources are dedicated to channel estimation and control signaling, the effective SNR and the payload that can be delivered are reduced with respect to the global achievable rate.

In [62] the overhead, incurred by channel estimation requirements, is accounted for by a percentage $\alpha$ which should grow, at least, linearly with the cluster size, up to a maximum value, to prevent it from being greater than 100 %. In that work, the SNR and the rate were effectively reduced by a factor of $\alpha$, getting $\mathtt{SNR}_{\text{eff}} = (1-\alpha)\,\mathtt{SNR}$ and $R_{\text{eff}} = (1-\alpha)\,R$.

In order to show the effect of the overhead on the achievable rate, in Figure 4.12

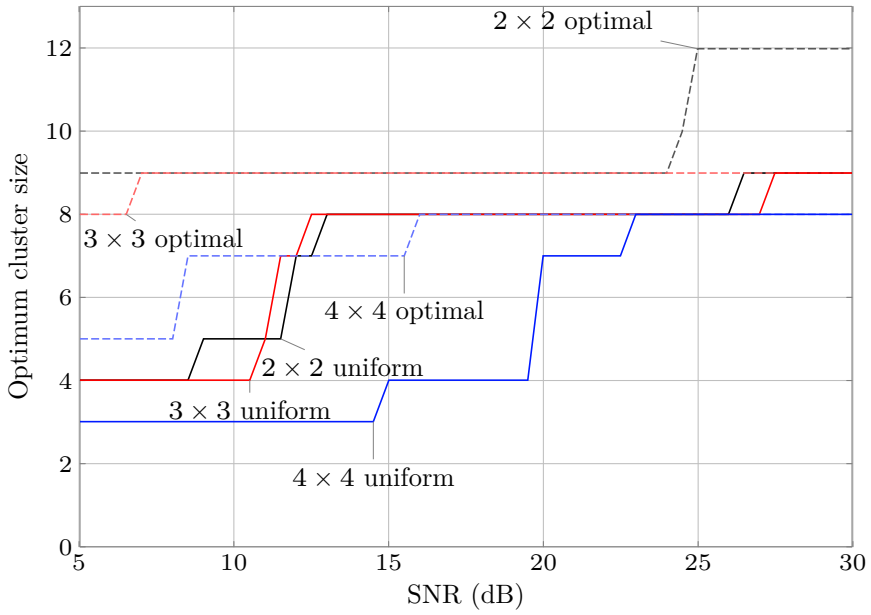


Figure 4.11: Optimum cluster size as a function of the SNR, for $\gamma = 3.8$ and different antenna configurations.

a very conservative approach is adopted, in which the value of the reduction factor $\alpha$ scales linearly with the cluster size $M$, up to a maximum of 10 % for a cluster size of 19.

Figure 4.12 shows the comparison of considering and not considering the overhead. It can be seen that even with a small amount of overhead, increasing values of $M$ lead to a worse performance.

Moreover, it should be stressed that the actual definition of signaling overhead and its management is usually delegated to the operator implementation, and this is seldom defined in the standards. Thus, its quantitative effect can change considerably depending on how the overhead is defined.

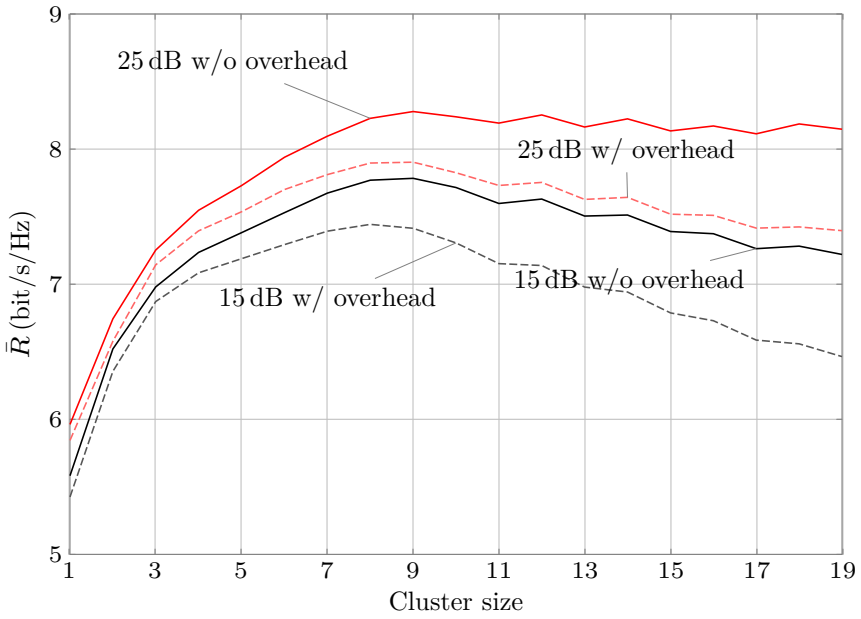


Figure 4.12: Mean achievable rate and payload rate as a function of the cluster size $M$ with different SNRs, for $r = 2$, $t = 2$, and $\gamma = 3.8$.

# Appendix A

# Derivation of $Z_i$

Using the change of variable

$$v = \frac{u}{R_{\text{cell}}} \tag{A.1}$$

in (4.38), it becomes

$$Z_i = \int_0^1 \log\left(\frac{v^{-\gamma}}{\frac{\sigma_i^2}{P_{\max} R_{\text{cell}}^{-\gamma}} + M_{\text{eq},i}\left(\bar{d}_i - v\right)^{\gamma}}\right) 2v\mathrm{d}v \tag{A.2}$$

Recall the definition of the SNR $\rho$ in (3.25), then

$$\begin{aligned} Z_i &= \int_0^1 \log\left(\frac{v^{-\gamma}}{\frac{1}{\rho} + M_{\text{eq},i}\left(\bar{d}_i - v\right)^{-\gamma}}\right) 2v\mathrm{d}v \\ &= \underbrace{2\int_0^1 \log\left(\frac{1}{\frac{1}{\rho} + M_{\text{eq},i}\left(\bar{d}_i - v\right)^{-\gamma}}\right) v\mathrm{d}v}_{\texttt{I}} \underbrace{-2\gamma\int_0^1 \log\left(v\right) v\mathrm{d}v}_{\texttt{II}} \end{aligned} \tag{A.3}$$

The term `II` in (A.3) is evaluated using (2.723) from [36], namely

$$\int v\log\left(v\right)\mathrm{d}v = v^2\left(\frac{\log\left(v\right)}{2} - \frac{1}{4}\right) \tag{A.4}$$

Using the change of variable

$$w = \bar{d}_i - v \tag{A.5}$$

in the term I of (A.3), it becomes

$$\begin{aligned}(\mathtt{I}) &= -\int_{\bar{d}_i}^{\bar{d}_i-1} \log\left(\frac{\rho}{1+M_{\mathrm{eq},i}\rho w^{-\gamma}}\right)\left(\bar{d}_i - w\right)\mathrm{d}w \\ &= \underbrace{\int_{\bar{d}_i-1}^{\bar{d}_i} \log\left(\rho\right)\left(\bar{d}_i - w\right)\mathrm{d}w}_{\mathtt{III}} + \underbrace{\int_{\bar{d}_i-1}^{\bar{d}_i} \log\left(\frac{1}{1+M_{\mathrm{eq},i}\rho w^{-\gamma}}\right)\left(\bar{d}_i - w\right)\mathrm{d}w}_{\mathtt{IV}}\end{aligned} \tag{A.6}$$

The term III of (A.6) is straightforward to calculate

$$\int_{\bar{d}_i-1}^{\bar{d}_i} \log\left(\rho\right)\left(\bar{d}_i - w\right)\mathrm{d}w = \log\left(\rho\right) \tag{A.7}$$

On the other hand, the term IV in (A.4) can be computed using the following result from [61]

$$\begin{aligned}\int_{\bar{d}_i-1}^{\bar{d}_i} \log\left(\frac{1}{1+M_{\mathrm{eq},i}\rho w^{-\gamma}}\right)\left(\bar{d}_i - w\right)\mathrm{d}w = w\Bigg[&\frac{2\bar{d}_i - w}{2}\log\left(\frac{w^{\gamma}}{M_{\mathrm{eq},i}\rho + w^{\gamma}}\right) \\ &- \bar{d}_i\gamma\,{}_2\mathrm{F}_1\left(1, \frac{1}{\gamma}; \frac{\gamma+1}{\gamma}; \frac{-w^{\gamma}}{M_{\mathrm{eq},i}\rho}\right) \\ &+ \frac{w\gamma}{4}\,{}_2\mathrm{F}_1\left(1, \frac{2}{\gamma}; \frac{\gamma+2}{\gamma}; \frac{-w^{\gamma}}{M_{\mathrm{eq},i}\rho}\right)\Bigg]\end{aligned} \tag{A.8}$$

where

$${}_2\mathrm{F}_1\left(a, b; c; z\right) = \frac{\Gamma\left(c\right)}{\Gamma\left(b\right)\Gamma\left(c-b\right)}\int_0^1 \frac{x^{b-1}\left(1-x\right)^{c-b-1}}{\left(1-x\right)^{a}}\mathrm{d}x \tag{A.9}$$

is the hypergeometric function.

Combining the previous, $Z_i$ can be expressed as

$$\begin{aligned} Z_i = &\frac{\gamma}{2} + \log(\rho) + \bar{d}_i^2 \log\left(\frac{\bar{d}_i^\gamma}{M_{\mathrm{eq},i}\rho + \bar{d}_i^\gamma}\right) \\ &- 2\bar{d}_i^2\gamma\,{}_2\mathrm{F}_1\left(1, \frac{1}{\gamma}; \frac{\gamma+1}{\gamma}; \frac{-\bar{d}_i^\gamma}{M_{\mathrm{eq},i}\rho + \bar{d}_i^\gamma}\right) \\ &+ \frac{\bar{d}_i^2}{2}\gamma\,{}_2\mathrm{F}_1\left(1, \frac{2}{\gamma}; \frac{\gamma+2}{\gamma}; \frac{-\bar{d}_i^\gamma}{M_{\mathrm{eq},i}\rho + \bar{d}_i^\gamma}\right) \\ &- \left(\bar{d}_i^2 - 1\right)\log\left(\frac{\left(\bar{d}_i - 1\right)^\gamma}{M_{\mathrm{eq},i}\rho + \left(\bar{d}_i - 1\right)^\gamma}\right) \\ &+ 2\bar{d}_i\left(\bar{d}_i - 1\right)\gamma\,{}_2\mathrm{F}_1\left(1, \frac{1}{\gamma}; \frac{\gamma+1}{\gamma}; \frac{-\left(\bar{d}_i - 1\right)^\gamma}{M_{\mathrm{eq},i}\rho}\right) \\ &- \frac{\left(\bar{d}_i - 1\right)^2}{2}\gamma\,{}_2\mathrm{F}_1\left(1, \frac{2}{\gamma}; \frac{\gamma+2}{\gamma}; \frac{-\left(\bar{d}_i - 1\right)^\gamma}{M_{\mathrm{eq},i}\rho}\right) \end{aligned} \tag{A.10}$$

# Appendix B

# Characterization of $\theta_{\text{th}}$

In this chapter, a brief analysis of the threshold $\theta_{\text{th}}$ is offered in order to show its dependence on some of the scenario parameters, for instance:

- Number of antennas of the MIMO configuration.
- SNR of the system.
- Cluster size.
- Path loss exponent $\gamma$.

Figures B.1 through B.4 show this dependence for a series of combinations of parameters.

First, Figure B.3 and Figure B.4 show how the threshold is consistently independent from the SNR, except for very low values of it.

For increasing values of the path loss exponent, the threshold increases as well, as it can be seen in Figure B.1 and Figure B.2. A higher path loss exponent translates into a lower level of interference between adjacent cells, in which case coordination may not help at all, so each BS better serves its own users independently. This is the reason for a higher threshold, which implies that less users will select BD as their preferred transmission strategy.

Another interesting characteristic that is clear in Figure B.2 and Figure B.4 is how the number of antennas plays no role in the threshold.

These two suggestions mean the advantages that MIMO has to offer have no influence on the value of the $\theta_{\text{th}}$, and it should depend mainly on the propagation characteristics of the channel.

This claim can be supported by Figure B.1 and Figure B.3, which show the behavior of the threshold with the cluster size, and by the already mentioned dependence on the

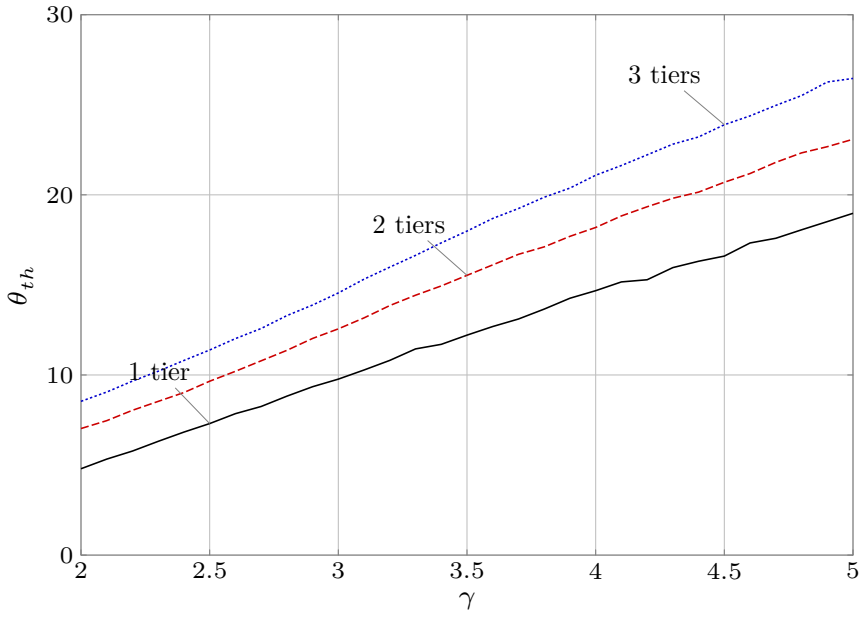


Figure B.1: Threshold as a function of the path loss exponent, for different cluster sizes, for an SNR of 15 dB.

path loss exponent. Cluster size is represented by the number of hexagonal tiers that form the cluster, so that 1 tiers is a 7 cells cluster, 2 tiers is a 19 cells cluster, and 3 tiers corresponds to a 37 cells cluster.

Similarly to what happened with the path loss exponent, a bigger cluster means that cells within a cluster may be too far away from some users in the cluster, who may not benefit much from coordination. As observed with the path loss exponent $\gamma$, reducing the level of influence among the cells in the cluster increases the value of the threshold, in this case when the cluster considered grows in size. Again, this higher value of $\theta_{\text{th}}$ means that more users will select SU as their transmission strategy.

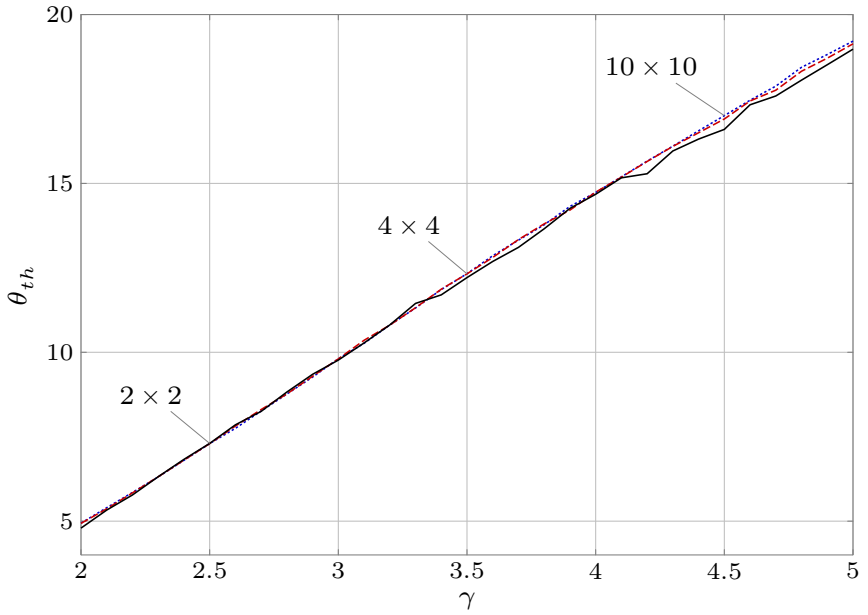


Figure B.2: Threshold as a function of the path loss exponent, for different MIMO configurations, for an SNR of 15 dB.

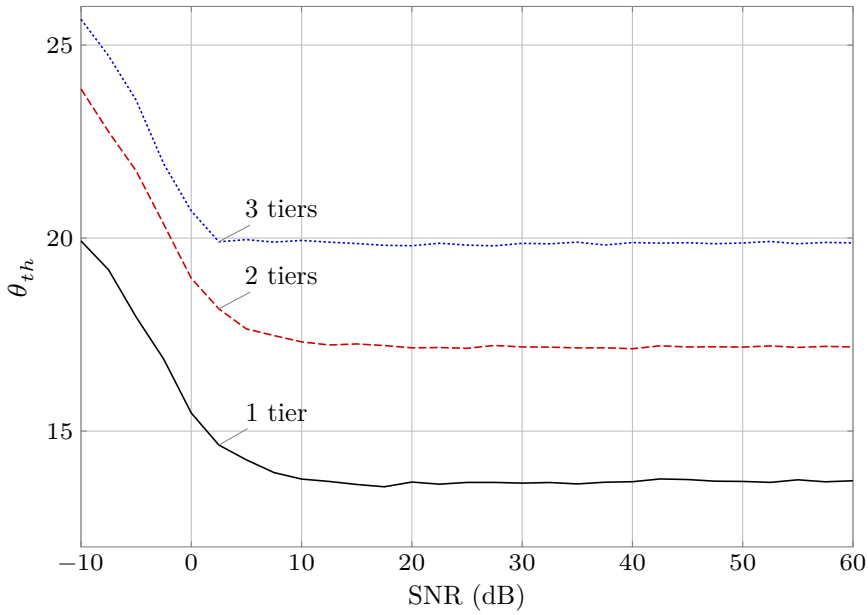


Figure B.3: Threshold as a function of the SNR, for different cluster sizes, for $\gamma = 3.8$.

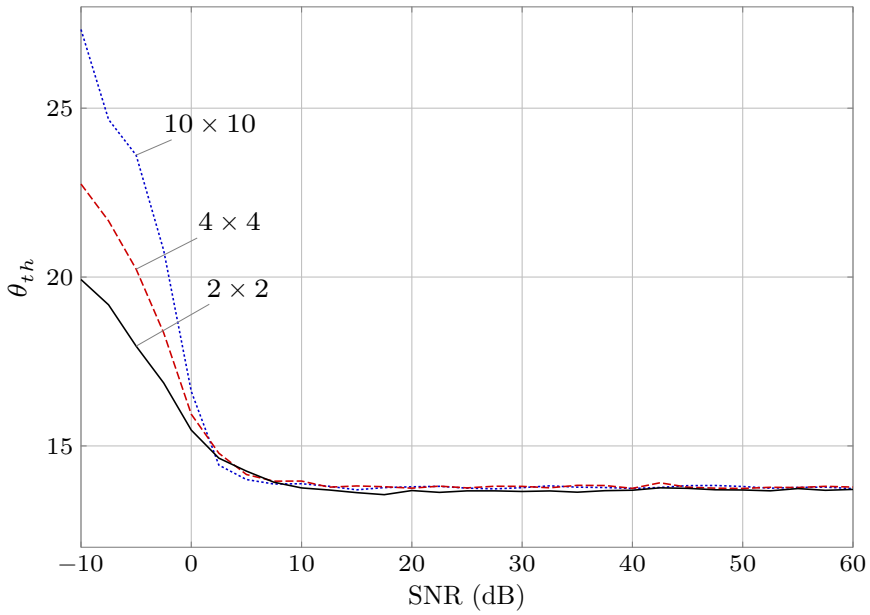


Figure B.4: Threshold as a function of the SNR, for different MIMO configurations, for $\gamma = 3.8$.

# Bibliography


[1] 3GPP. *3rd Generation Partnership Project; Technical Specification Group Radio Access Network; Coordinated multi-point operation for LTE physical layer aspects (Release 11)*. Tech. rep. 3GPP, Dec. 2011.

[2] 3GPP. *LTE*. Apr. 2014. URL: `http://www.3gpp.org/LTE`.

[3] 3GPP. *LTE-Advanced*. Apr. 2014. URL: `http://www.3gpp.org/LTE-Advanced`.

[4] 3GPP. *Multiple Input Multiple Output in UTRA (3GPP TR 25.876 version 7.0.0 Release 7)*. Tech. rep. 3GPP, Mar. 2007.

[5] Jeffrey G. Andrews et al. "What will 5G be?" In: *arXiv preprint arXiv:1405.2957* (2014).

[6] Paolo Baracca, Federico Boccardi, and Volker Braun. "A Dynamic Joint Clustering Scheduling Algorithm for Downlink CoMP Systems With Limited CSI". In: *2012 International Symposium on Wireless Communication Systems (ISWCS)*. 2012, pp. 830–834.

[7] Alan Barbieri et al. "Coordinated Downlink Multi-Point Communications in Heterogeneous Cellular Networks". In: *Information Theory and Applications Workshop (ITA), 2012*. Feb. 2012, pp. 7–16.

[8] Emil Björnson et al. "Cooperative Multicell Precoding: Rate Region Characterization and Distributed Strategies With Instantaneous and Statistical CSI". In: *IEEE Transactions on Signal Processing* 58.8 (Aug. 2010), pp. 4298–4310.

[9] Emil Björnson et al. "Optimality Properties, Distributed Strategies, and Measurement-Based Evaluation of Coordinated Multicell OFDMA Transmission". In: *IEEE Transactions on Signal Processing* 59.12 (Dec. 2011), pp. 6086–6101.

[10] Federico Boccardi and Howard Huang. "Optimum power allocation for the MIMO-BC zero-forcing precoder with per-antenna power constraints". In: *2006 40th Annual Conference on Information Sciences and Systems*. Mar. 2006, pp. 504–504.

[11] Tadilo E. Bogale and Luc Vandendorpe. "Robust Sum MSE Optimization for Downlink Multiuser MIMO Systems With Arbitrary Power Constraint: Generalized Duality Approach". In: *IEEE Transactions on Signal Processing* 60.4 (Apr. 2012), pp. 1862–1875.

[12] Tadilo E. Bogale and Luc Vandendorpe. “Weighted Sum Rate Optimization for Downlink Multiuser MIMO Coordinated Base Station Systems: Centralized and Distributed Algorithms”. In: *IEEE Transactions on Signal Processing* 60.4 (Apr. 2012), pp. 1876–1889.

[13] Stephen P. Boyd and Lieven Vandenberghe. *Convex optimization*. Cambridge university press, 2009.

[14] Guy Bresler, Dustin Cartwright, and David Tse. “Feasibility of Interference Alignment for the MIMO Interference Channel”. In: *IEEE Transactions on Information Theory* 60.9 (Sept. 2014), pp. 5573–5586.

[15] Richard L. Burden and J. Douglas Faires. *Numerical Analysis*. Cengage Learning, 2010.

[16] Viveck R. Cadambe and Syed A. Jafar. “Interference Alignment and Degrees of Freedom of the K -User Interference Channel”. In: *IEEE Transactions on Information Theory* 54.8 (Aug. 2008), pp. 3425–3441.

[17] Giuseppe Caire and Shlomo Shamai Shitz. “On achievable rates in a multi-antenna broadcast downlink”. In: *Proc. 38th Annu. Allerton Conf. Communication, Control and Computing*. 2000, pp. 1188–1193.

[18] Giuseppe Caire and Shlomo Shamai Shitz. “On the Achievable throughput of a Multiantenna Gaussian Broadcast Channel”. In: *IEEE Transactions on Information Theory* 49.7 (July 2003), pp. 1691–1706.

[19] Dorra Ben Cheikh et al. “SIR Distribution Analysis in Cellular Networks Considering the Joint Impact of Path-Loss, Shadowing and Fast Fading”. In: *EURASIP Journal on Wireless Communications and Networking* 2011.1 (2011), pp. 1–10.

[20] Woon Hau Chin, Zhong Fan, and Russell Haines. “Emerging technologies and research challenges for 5G wireless networks”. In: *Wireless Communications, IEEE* 21.2 (Apr. 2014), pp. 106–112.

[21] Wan Choi and Jeffrey G. Andrews. “Downlink performance and capacity of distributed antenna systems in a multicell environment”. In: *IEEE Transactions on Wireless Communications* 6.1 (Jan. 2007), pp. 69–73.

[22] John M. Cioffi. *EE379C - Advanced Digital Communication - Class Notes - Chapter 4*, p. 307.

[23] Roberto Corvaja, Juan José García Fernández, and Ana García Armada. “Achievable Rate and Fairness in Coordinated Base Station Transmission”. In: *Communications Letters, IEEE* 18.4 (Apr. 2014), pp. 584–587.

[24] Roberto Corvaja, Juan José García Fernández, and Ana García Armada. “Mean Achievable Rates in Clustered Coordinated Base Station Transmission With Block Diagonalization”. In: *IEEE Transactions on Communications* 61.8 (Aug. 2013), pp. 3483–3493.

[25] Thomas M Cover and Joy A Thomas. *Elements of information theory*. John Wiley & Sons, 2012.

[26] Ying Cui, Qingqing Huang, and Vincent K. N. Lau. "Queue-Aware Dynamic Clustering and Power Allocation for Network MIMO Systems via Distributed Stochastic Learning". In: *IEEE Transactions on Signal Processing* 59.3 (Mar. 2011), pp. 1229–1238.

[27] Ana García Armada, Matilde Sánchez-Fernández, and Roberto Corvaja. "Constrained Power Allocation Schemes for Coordinated Base Station Transmission Using Block Diagonalization". In: *EURASIP Journal on Wireless Communications and Networking* 2011.1 (2011), pp. 1–14.

[28] Ana García Armada et al. "MMSE Precoding for Downlink Coordinated Base Station Transmission". In: *Vehicular Technology Conference (VTC Spring), 2011 IEEE 73rd*. May 2011, pp. 1–5.

[29] Juan José García Fernández et al. "Adaptive Block Diagonalization and User Scheduling With Out of Cluster Interference". In: *European Wireless 2014; 20th European Wireless Conference; Proceedings of*. May 2014, pp. 1–6.

[30] David Gesbert et al. "Adaptation, Coordination, and Distributed Resource Allocation in Interference-Limited Wireless Networks". In: *Proceedings of the IEEE* 95.12 (Dec. 2007), pp. 2393–2409.

[31] David Gesbert et al. "Multi-Cell MIMO Cooperative Networks: A New Look at Interference". In: *IEEE Journal on Selected Areas in Communications* 28.9 (Dec. 2010), pp. 1380–1408.

[32] David Gesbert et al. "Shifting the MIMO Paradigm". In: *Signal Processing Magazine, IEEE* 24.5 (Sept. 2007), pp. 36–46.

[33] Jie Gong et al. "Joint Scheduling and Dynamic Clustering in Downlink Cellular Networks". In: *Global Telecommunications Conference (GLOBECOM 2011), 2011 IEEE*. 2011, pp. 1–5.

[34] Tiangao Gou and Syed A. Jafar. "Degrees of Freedom of the K User M ×N MIMO Interference Channel". In: *IEEE Transactions on Information Theory* 56.12 (Dec. 2010), pp. 6040–6057.

[35] Tiangao Gou, Chenwei Wang, and Syed A. Jafar. "Aiming Perfectly in the Dark-Blind Interference Alignment Through Staggered Antenna Switching". In: *IEEE Transactions on Signal Processing* 59.6 (June 2011), pp. 2734–2744.

[36] Izrail Solomonovich Gradshteyn and Iosif Moiseevich Ryzhik. *Table of Integrals, Series, and Products*. Academic Press, 2000.

[37] Michael C. Grant and Stephen P. Boyd. *CVX: Matlab Software for Disciplined Convex Programming, version 2.1*. `http://cvxr.com/cvx`. Mar. 2014.

[38] Michael C. Grant and Stephen P. Boyd. "Graph implementations for nonsmooth convex programs". In: *Recent Advances in Learning and Control*. Ed. by Vincent D. Blondel, Stephen P. Boyd, and Hidenori Kimura. Lecture Notes in Control and Information Sciences. `http://stanford.edu/~boyd/graph_dcp.html`. Springer-Verlag Limited, 2008, pp. 95–110.

[39] Shiwen He et al. “Coordinated Multicell Multiuser Precoding for Maximizing Weighted Sum Energy Efficiency”. In: *IEEE Transactions on Signal Processing* 62.3 (Feb. 2014), pp. 741–751.

[40] Bengt Holter. “On the capacity of the MIMO channel: A tutorial introduction”. In: *Proc. IEEE Norwegian Symposium on Signal Processing*. 2001, pp. 167–172.

[41] Mingyi Hong et al. “Joint Base Station Clustering and Beamformer Design for Partial Coordinated Transmission in Heterogeneous Networks”. In: *IEEE Journal on Selected Areas in Communications* 31.2 (2013), pp. 226–240.

[42] Kianoush Hosseini, Wei Yu, and Raviraj S. Adve. “Cluster based coordinated beamforming and power allocation for MIMO heterogeneous networks”. In: *2013 13th Canadian Workshop on Information Theory (CWIT)*. June 2013, pp. 96–101.

[43] Howard Huang et al. “Increasing Downlink Cellular Throughput With Limited Network MIMO Coordination”. In: *IEEE Transactions on Wireless Communications* 8.6 (June 2009), pp. 2983–2989.

[44] Yongming Huang et al. “Distributed Multicell Beamforming With Limited Intercell Coordination”. In: *IEEE Transactions on Signal Processing* 59.2 (Feb. 2011), pp. 728–738.

[45] ITU-R. *Detailed specifications of the terrestrial radio interfaces of International Mobile Telecommunications-Advanced (IMT-Advanced), Recommendation ITU-R M.2012-1*. Tech. rep. ITU-R, Feb. 2014.

[46] Syed A. Jafar. “Blind Interference Alignment”. In: *IEEE Journal of Selected Topics in Signal Processing* 6.3 (June 2012), pp. 216–227.

[47] Syed A. Jafar. “Interference Alignment — A New Look at Signal Dimensions in a Communication Network”. In: *Foundations and Trends® in Communications and Information Theory* 7.1 (2010), pp. 1–134. URL: http://dx.doi.org/10.1561/0100000047.

[48] Syed A. Jafar. “Topological Interference Management Through Index Coding”. In: *IEEE Transactions on Information Theory* 60.1 (Jan. 2014), pp. 529–568.

[49] Syed A. Jafar, Gerard J. Foschini, and Andrea J. Goldsmith. “Phantomnet: Exploring optimal multicellular multiple antenna systems”. In: *EURASIP Journal on Applied Signal Processing* 2004 (2004), pp. 591–604.

[50] Syed A. Jafar and Shlomo Shamai Shitz. “Degrees of Freedom Region of the MIMO X Channel”. In: *IEEE Transactions on Information Theory* 54.1 (Jan. 2008), pp. 151–170.

[51] Nihar Jindal, Sriram Vishwanath, and Andrea J. Goldsmith. “On the duality of Gaussian multiple-access and broadcast channels”. In: *IEEE Transactions on Information Theory* 50.5 (May 2004), pp. 768–783.

[52] Nihar Jindal, Sriram Vishwanath, and Andrea J. Goldsmith. “On the duality of multiple-access and broadcast channels”. In: *Proceedings of the Annual Allerton Conference on Communication Control and Computing*. Vol. 39. 2. The University; 1998. 2001, pp. 1026–1035.

[53] M. Kemal Karakayali, Gerard J. Foschini, and Reinaldo A. Valenzuela. “Network Coordination for Spectrally Efficient Communications in Cellular Systems”. In: *Wireless Communications, IEEE* 13.4 (Aug. 2006), pp. 56–61.

[54] M. Kemal Karakayali et al. “On the maximum common rate achievable in a coordinated network”. In: *2006. ICC'06. IEEE International Conference on Communications*. Vol. 9. IEEE. June 2006, pp. 4333–4338.

[55] Saeed Kaviani and Witold A. Krzymień. “Multicell Scheduling in Network MIMO”. In: *Global Telecommunications Conference (GLOBECOM 2010), 2010 IEEE*. Dec. 2010, pp. 1–5.

[56] Kyeongjun Ko and Jungwoo Lee. “Multiuser MIMO User Selection Based on Chordal Distance”. In: *IEEE Transactions on Communications* 60.3 (Mar. 2012), pp. 649–654.

[57] Tilak Rajesh Lakshmana, Carmen Botella, and Tommy Svensson. “Partial Joint Processing with Efficient Backhauling in Coordinated Multipoint Networks”. In: *Vehicular Technology Conference (VTC Spring), 2012 IEEE 75th*. 2012, pp. 1–5.

[58] Sina Lashgari, Amir S. Avestimehr, and Changho Suh. “Linear Degrees of Freedom of the X-Channel With Delayed CSIT”. In: *IEEE Transactions on Information Theory* 60.4 (Apr. 2014), pp. 2180–2189.

[59] Sang-Rim Lee et al. “Capacity Analysis of Distributed Antenna Systems in a Composite Fading Channel”. In: *IEEE Transactions on Wireless Communications* 11.3 (Mar. 2012), pp. 1076–1086.

[60] Wei Liu, Soon Xin Ng, and Lajos Hanzo. “Multicell Cooperation Based SVD Assisted Multi-User MIMO Transmission”. In: *Vehicular Technology Conference, 2009. VTC Spring 2009. IEEE 69th*. Apr. 2009, pp. 1–5.

[61] Wolfram Alpha LLC. *Wolfram Alpha*. 2014. URL: `http://www.wolframalpha.com`.

[62] Angel Lozano, Robert W. Heath Jr., and Jeffrey G. Andrews. “Fundamental Limits of Cooperation”. In: *IEEE Transactions on Information Theory* 59.9 (2013), pp. 5213–5226.

[63] I-Tai Lu and Jialing Li. “Novel MMSE precoder and decoder designs subject to per-antenna power constraint for uplink multiuser MIMO systems”. In: *2009. ICSPCS 2009. 3rd International Conference on Signal Processing and Communication Systems*. Sept. 2009, pp. 1–5.

[64] Mohammad Ali Maddah-Ali, Amir Keyvan Khandani, and Abolfazl Sayed Motahari. *Communication over X channel: Signalling and multiplexing gain*. Citeseer, 2006.

[65] Jung-Min Moon and Dong-Ho Cho. “Inter-Cluster Interference Management Based on Cell-Clustering in Network MIMO Systems”. In: *Vehicular Technology Conference (VTC Spring), 2011 IEEE 73rd*. May 2011, pp. 1–6.

[66] Sung-Hyun Moon et al. “Joint User Scheduling and Adaptive Intercell Interference Cancelation for MISO Downlink Cellular Systems”. In: *IEEE Transactions on Vehicular Technology* 62.1 (Jan. 2013), pp. 172–181.

[67] Máximo Morales-Céspedes et al. “Blind Interference Alignment for Cellular Networks”. In: *IEEE Transactions on Signal Processing* 63.1 (Jan. 2015), pp. 41–56.

[68] Chris T. K. Ng and Howard Huang. “Linear Precoding in Cooperative MIMO Cellular Networks with Limited Coordination Clusters”. In: *IEEE Journal on Selected Areas in Communications* 28.9 (Dec. 2010), pp. 1446–1454.

[69] Agisilaos Papadogiannis and George C. Alexandropoulos. “The Value of Dynamic Clustering of Base Stations for Future Wireless Networks”. In: *2010 IEEE International Conference on Fuzzy Systems (FUZZ)*. 2010, pp. 1–6.

[70] Agisilaos Papadogiannis, David Gesbert, and Eric Hardouin. “A Dynamic Clustering Approach in Wireless Networks with Multi-Cell Cooperative Processing”. In: *2008. ICC ’08. IEEE International Conference on Communications*. May 2008, pp. 4033–4037.

[71] Agisilaos Papadogiannis et al. “Efficient Selective Feedback Design for Multicell Cooperative Networks”. In: *IEEE Transactions on Vehicular Technology* 60.1 (Jan. 2011), pp. 196–205.

[72] Athanasios Papoulis. *The Fourier Integral and its Applications*. Mc Graw-Hill, 1962.

[73] Benoit Pijcke et al. “An Analytical Model for the Intercell Interference Power in the Downlink of Wireless Cellular Networks”. In: *EURASIP Journal on Wireless Communications and Networking* 2011.1 (2011), pp. 1–20.

[74] Sean A. Ramprashad, Giuseppe Caire, and Haralabos C. Papadopoulos. “A Joint Scheduling and Cell Clustering Scheme for MU-MIMO Downlink with Limited Coordination”. In: *2010 IEEE International Conference on Communications (ICC)*. May 2010, pp. 1–6.

[75] Martin Schubert and Holger Boche. “Joint ’dirty paper’ pre-coding and downlink beamforming”. In: *2002 IEEE Seventh International Symposium on Spread Spectrum Techniques and Applications*. Vol. 2. 2002, pp. 536–540.

[76] Shlomo Shamai Shitz and Benjamin M. Zaidel. “Enhancing the Cellular Downlink Capacity via Co-processing at the Transmitting End”. In: *Vehicular Technology Conference, 2001. VTC 2001 Spring. IEEE VTS 53rd*. Vol. 3. 2001, pp. 1745–1749.

[77] Zukang Shen et al. “Low Complexity User Selection Algorithms for Multiuser MIMO Systems With Block Diagonalization”. In: *IEEE Transactions on Signal Processing* 54.9 (2006), pp. 3658–3663.

[78] Qingjiang Shi et al. “An Iteratively Weighted MMSE Approach to Distributed Sum-Utility Maximization for a MIMO Interfering Broadcast Channel”. In: *IEEE Transactions on Signal Processing* 59.9 (Sept. 2011), pp. 4331–4340.

[79] Shuying Shi et al. “MMSE Optimization with Per-Base-Station Power Constraints for Network MIMO Systems”. In: *2008. ICC ’08. IEEE International Conference on Communications*. May 2008, pp. 4106–4110.

[80] Seijoon Shim et al. “Block Diagonalization for Multi-User MIMO With Other-Cell Interference”. In: *IEEE Transactions on Wireless Communications* 7.7 (July 2008), pp. 2671–2681.

[81] Illsoo Sohn, Hyoungjoo Lee, and Kwang Bok Lee. “Generalized MMSE beamforming for multicell MIMO systems with random user geometry and channel feedback latency”. In: *EURASIP Journal on Wireless Communications and Networking* 2014.1, 86 (2014), pp. 1–10. URL: `http://dx.doi.org/10.1186/1687-1499-2014-86`.

[82] Quentin H. Spencer, A. Lee Swindlehurst, and Martin Haardt. “Zero-Forcing Methods for Downlink Spatial Multiplexing in Multiuser MIMO Channels”. In: *IEEE Transactions on Signal Processing* 52.2 (Feb. 2004), pp. 461–471.

[83] Quentin H. Spencer et al. “An introduction to the multi-user MIMO downlink”. In: *Communications Magazine, IEEE* 42.10 (Oct. 2004), pp. 60–67.

[84] Veljko Stankovic and Martin Haardt. “Generalized Design of Multi-User MIMO Precoding Matrices”. In: *IEEE Transactions on Wireless Communications* 7.3 (Mar. 2008), pp. 953–961.

[85] Huan Sun, Wei Fang, and Lin Yang. “A Novel Precoder Design for Coordinated Multipoint Downlink Transmission”. In: *Vehicular Technology Conference (VTC Spring), 2011 IEEE 73rd*. May 2011, pp. 1–5.

[86] Charles Swannack, Elif Uysal-Biyikoglu, and Gregory W. Wornell. “Finding NEMO: near mutually orthogonal sets and applications to MIMO broadcast scheduling”. In: *2005 International Conference on Wireless Networks, Communications and Mobile Computing*. Vol. 2. June 2005, pp. 1035–1040.

[87] Antonia M Tulino and Sergio Verdú. “Random Matrix Theory and Wireless Communications”. In: *Foundations and Trends in Communications and Information Theory* 1.1 (June 2004), pp. 1–182.

[88] Sivarama Venkatesan, Angel Lozano, and Reinaldo Valenzuela. “Network MIMO: Overcoming intercell interference in indoor wireless systems”. In: *2007. ACSSC 2007. Conference Record of the Forty-First Asilomar Conference on Signals, Systems and Computers*. IEEE. 2007, pp. 83–87.

[89] Sriram Vishwanath, Nihar Jindal, and Andrea J. Goldsmith. "On the capacity of multiple input multiple output broadcast channels". In: *2002. ICC 2002. IEEE International Conference on Communications*. Vol. 3. 2002, pp. 1444–1450.

[90] Hanan Weingarten, Yossef Steinberg, and Shlomo Shamai Shitz. "The Capacity Region of the Gaussian Multiple-Input Multiple-Output Broadcast Channel". In: *IEEE Transactions on Information Theory* 52.9 (Sept. 2006), pp. 3936–3964.

[91] Ami Wiesel, Yonina C. Eldar, and Shlomo Shamai Shitz. "Zero-Forcing Precoding and Generalized Inverses". In: *IEEE Transactions on Signal Processing* 56.9 (Sept. 2008), pp. 4409–4418.

[92] Xinping Yi and Edward K.S. Au. "User Scheduling for Heterogeneous Multiuser MIMO Systems: A Subspace Viewpoint". In: *IEEE Transactions on Vehicular Technology* 60.8 (Oct. 2011), pp. 4004–4013.

[93] Taesang Yoo and Andrea J. Goldsmith. "On the Optimality of Multiantenna Broadcast Scheduling Using Zero-Forcing Beamforming". In: *IEEE Journal on Selected Areas in Communications* 24.3 (Mar. 2006), pp. 528–541.

[94] Wei Yu and John M. Cioffi. "Sum capacity of Gaussian vector broadcast channels". In: *IEEE Transactions on Information Theory* 50.9 (Sept. 2004), pp. 1875–1892.

[95] Wei Yu and John M. Cioffi. "Trellis precoding for the broadcast channel". In: *Global Telecommunications Conference, 2001. GLOBECOM'01. IEEE*. Vol. 2. IEEE. 2001, pp. 1344–1348.

[96] Jun Zhang et al. "Networked MIMO With Clustered Linear Precoding". In: *IEEE Transactions on Wireless Communications* 8.4 (Apr. 2009), pp. 1910–1921.

[97] Rui Zhang. "Cooperative Multi-Cell Block Diagonalization with Per-Base-Station Power Constraints". In: *IEEE Journal on Selected Areas in Communications* 28.9 (Dec. 2010), pp. 1435–1445.